Supporting Information

Synthesis, Characterization, Photophysics, and Anion Binding Properties of Gold(I) Acetylide Complexes with Amide Group

Hua-Yun Shi, Jie Qi, Zhen-Ze Zhao, Wen-Juan Feng, Yu-Hao Li, Lu Sun, Zhuo-Jia Lin, Hsiu-Yi Chao*

MOE Key Laboratory of Bioinorganic and Synthetic Chemistry, School of Chemistry and Chemical Engineering, Sun Yat-Sen University, Guangzhou 510275, P. R. China

Table S1. Crystallographic data for **3a**

Formula	$C_{33}H_{24}AuN_2O_3P$
M (g/mol)	724.48
cryst syst	Triclinic
space group	P –1
a (Å)	8.7748(18)
b (Å)	9.1491(18)
c (Å)	17.558(4)
α (°)	93.54(3)
β (°)	97.12(3)
γ (°)	98.33(3)
V (Å^3)	1379.4(5)
Z	2
D_c (g cm^{-3})	1.744
T (K)	173(2)
reflns collected	10395
indep reflns	5257
R_{int}	0.0385
R,[a] R_w[b] [I > 2σ(*I*)]	0.0345, 0.0854
GOF	0.768

[a]$R = \Sigma(|F_o| - |F_c|) / \Sigma|F_o|$. [b]$R_w = [\Sigma w(|F_o| - |F_c|)^2 / \Sigma w|F_o|2]^{1/2}$.

Table S2. Binding constants of **4a**−**4d** with anions in $CDCl_3$[a]

ligand	F^-	Cl^-	OAc^-	Br^-	I^-
4a	[b]	220.81±15.22	188.82±13.14	167.21±16.58	71.03±4.75
4b	[b]	97.15±7.7	54.22±3.04	46.74±7.30	31.56±2.12
4c	[b]	28.43±2.62	22.13±2.69	18.82±1.62	3.83±2.45
4d	[b]	33.13±1.64	20.53±1.27	19.1500±1.75	13.00±0.61

[a]Binding constants were determined by 1:1 model using nonlinear fitting methods.

[b]Chemical shifts were not suitable for accurate measurement of binding constant.

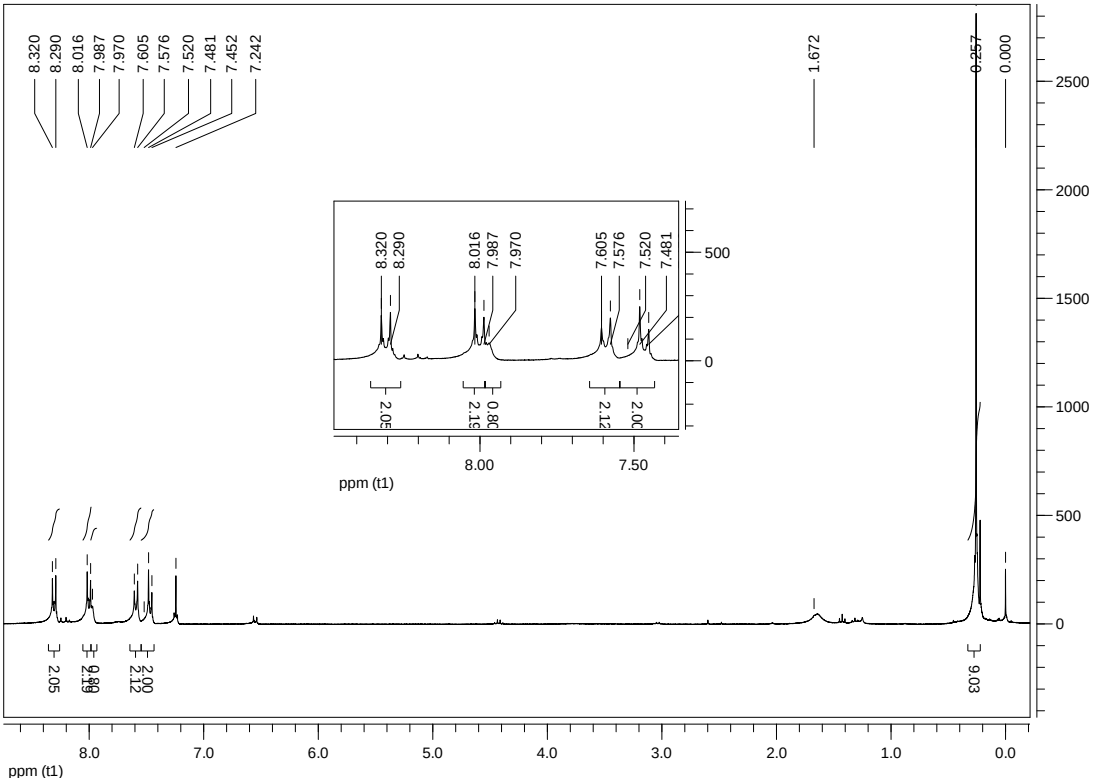

Figure S1. The ^{1}H NMR spectrum of **2a** in $CDCl_3$ at 298 K.

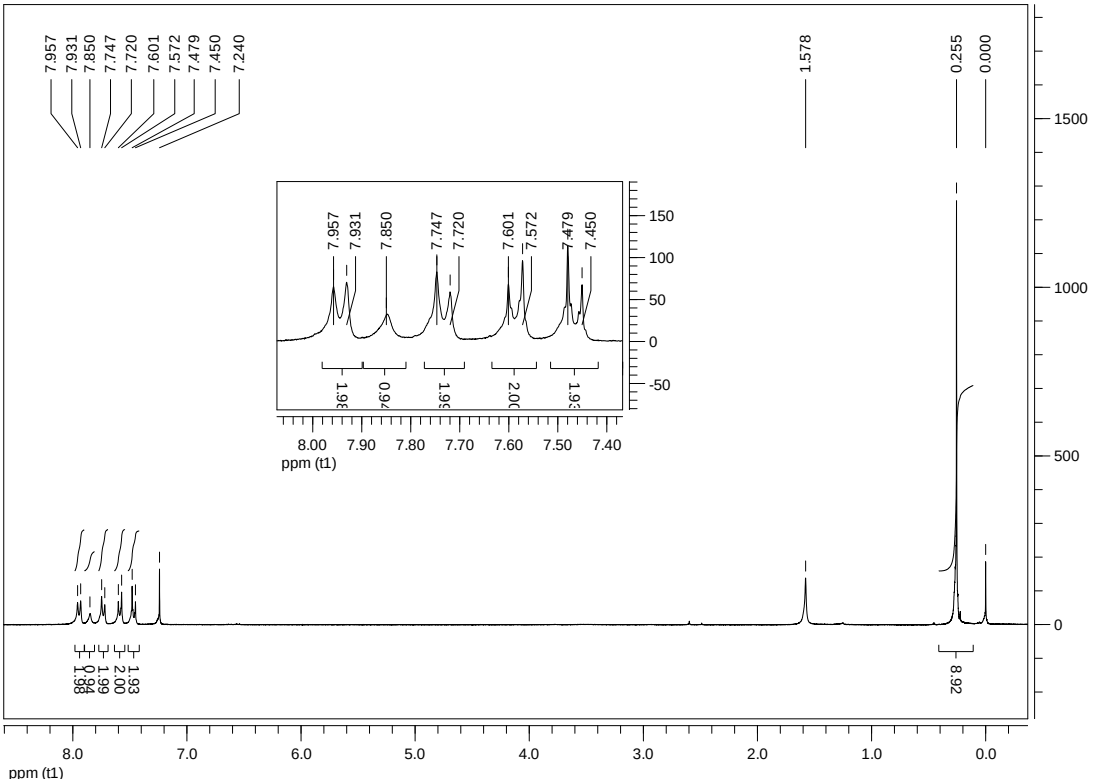

Figure S2. The ^{1}H NMR spectrum of **2b** in $CDCl_3$ at 298 K.

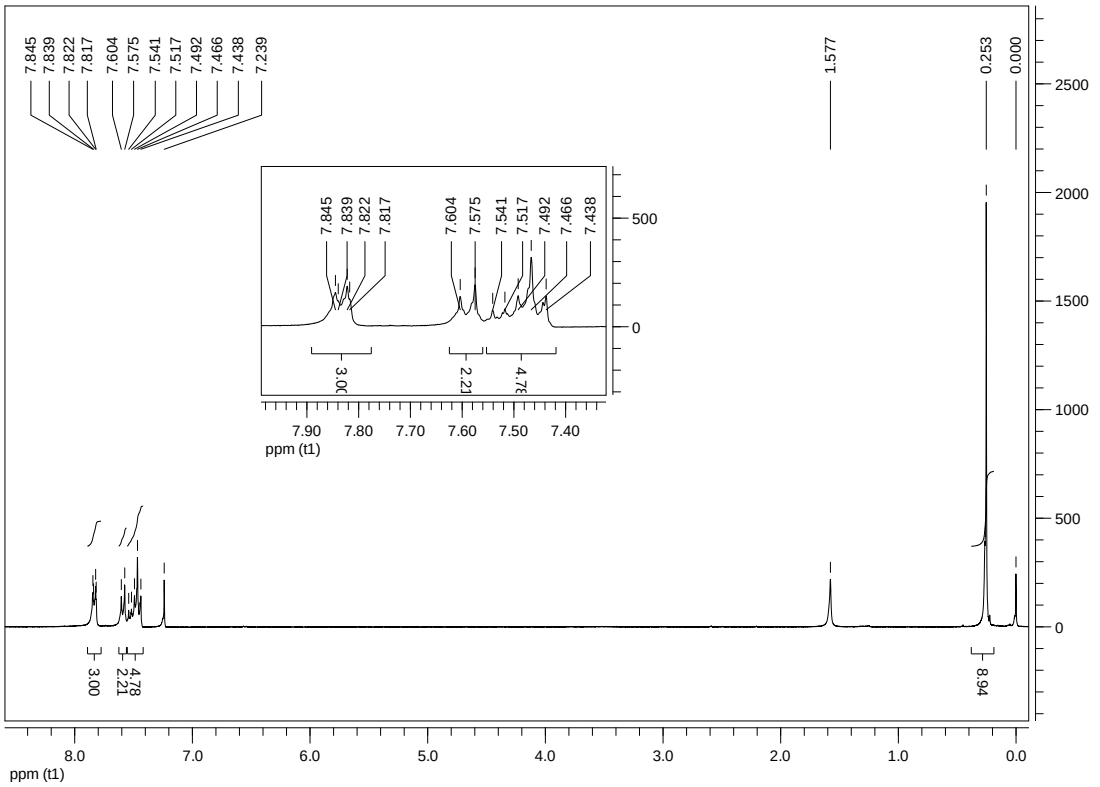

Figure S3. The ^{1}H NMR spectrum of **2c** in $CDCl_3$ at 298 K.

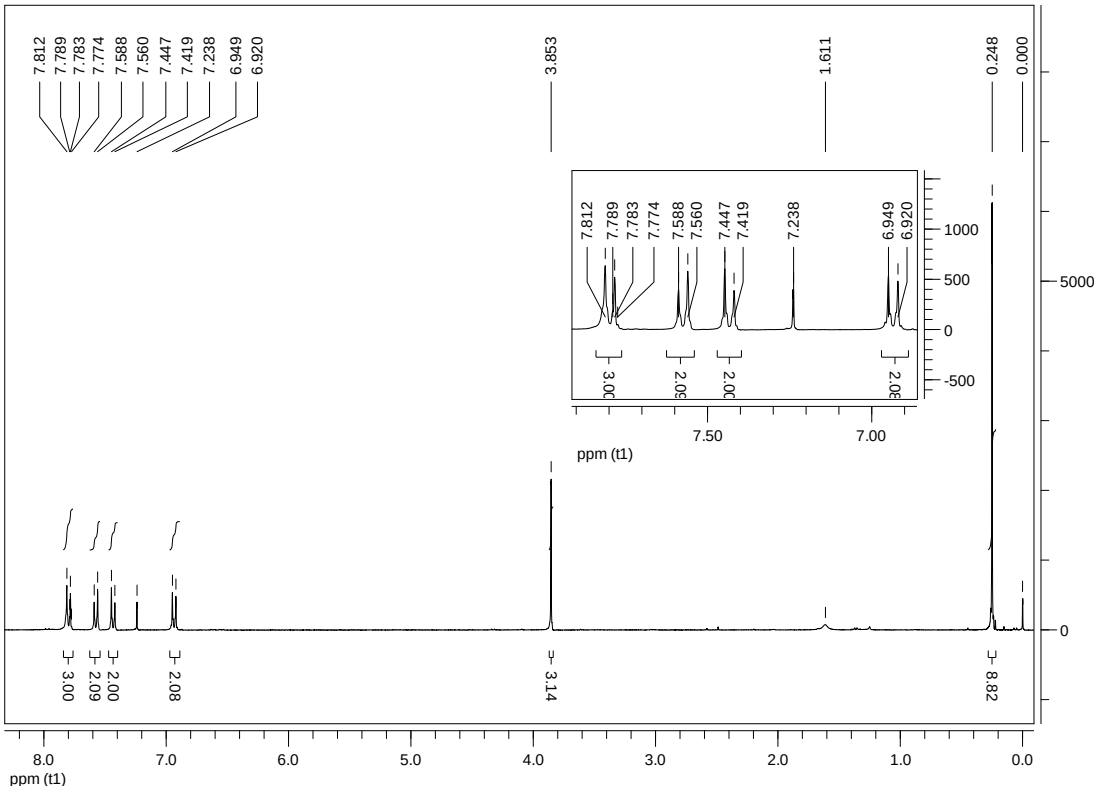

Figure S4. The ^{1}H NMR spectrum of **2d** in $CDCl_3$ at 298 K.

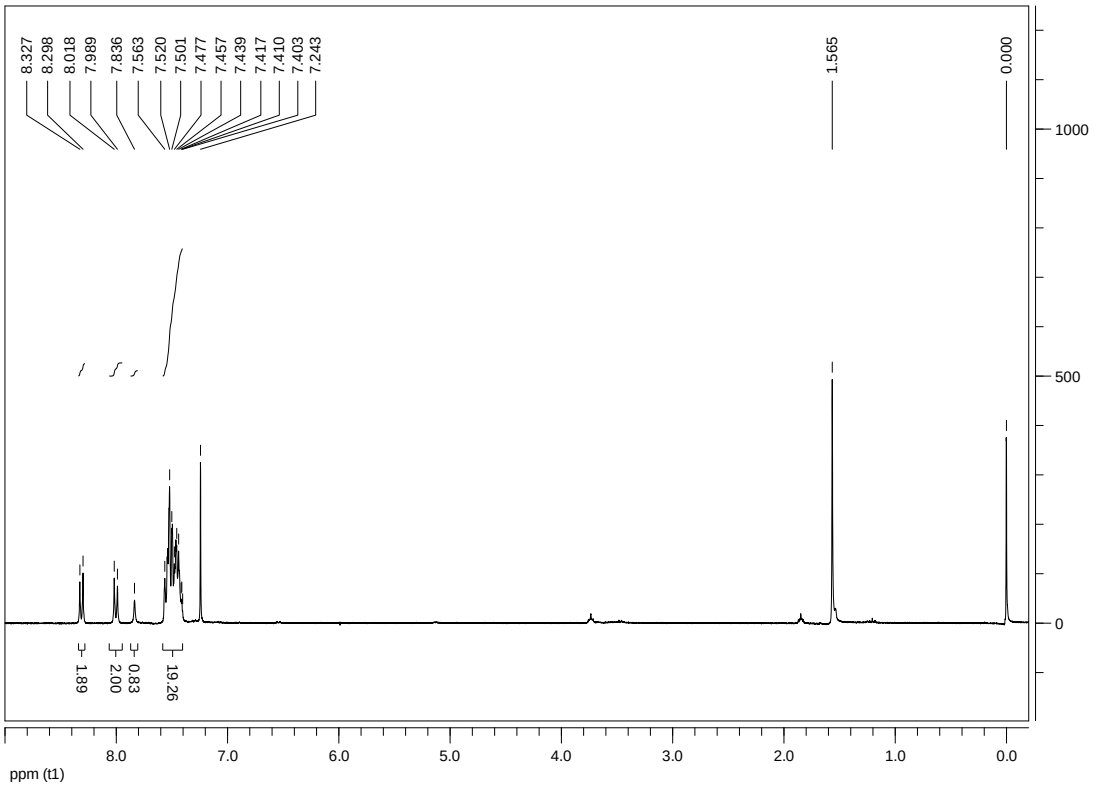

Figure S5. The ^{1}H NMR spectrum of **3a** in $CDCl_3$ at 298 K.

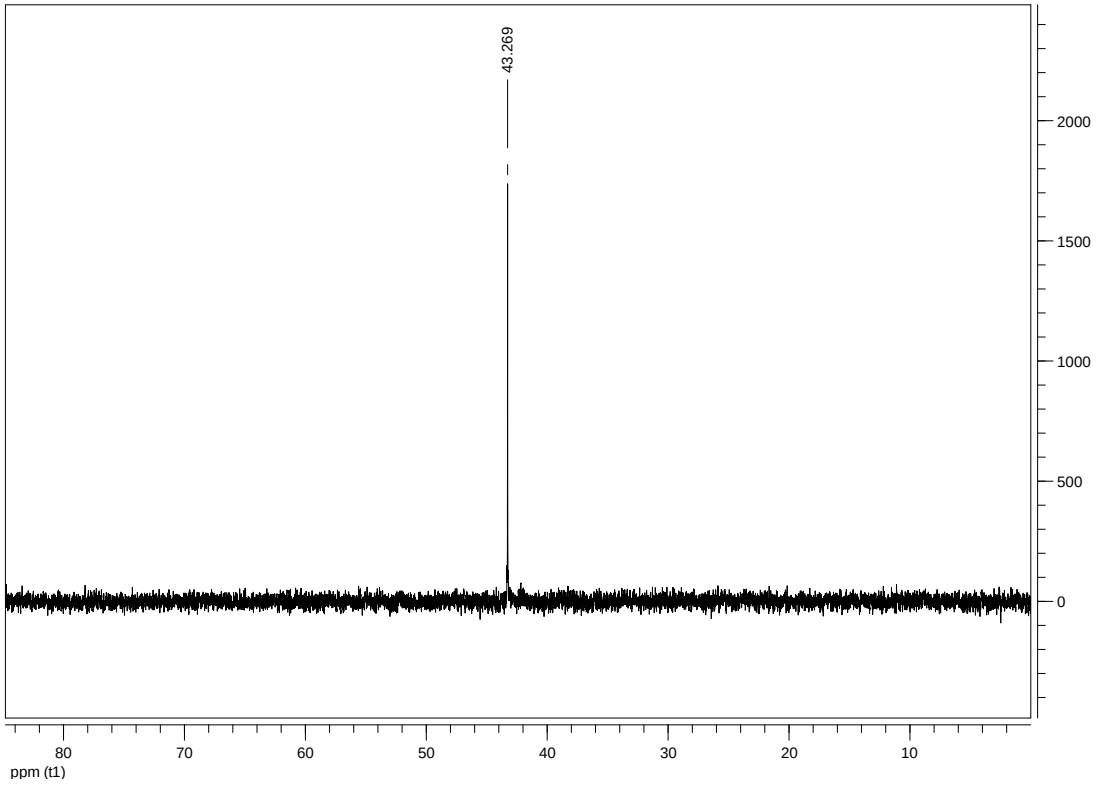

Figure S6. The ^{31}P NMR spectrum of **3a** in $CDCl_3$ at 298 K.

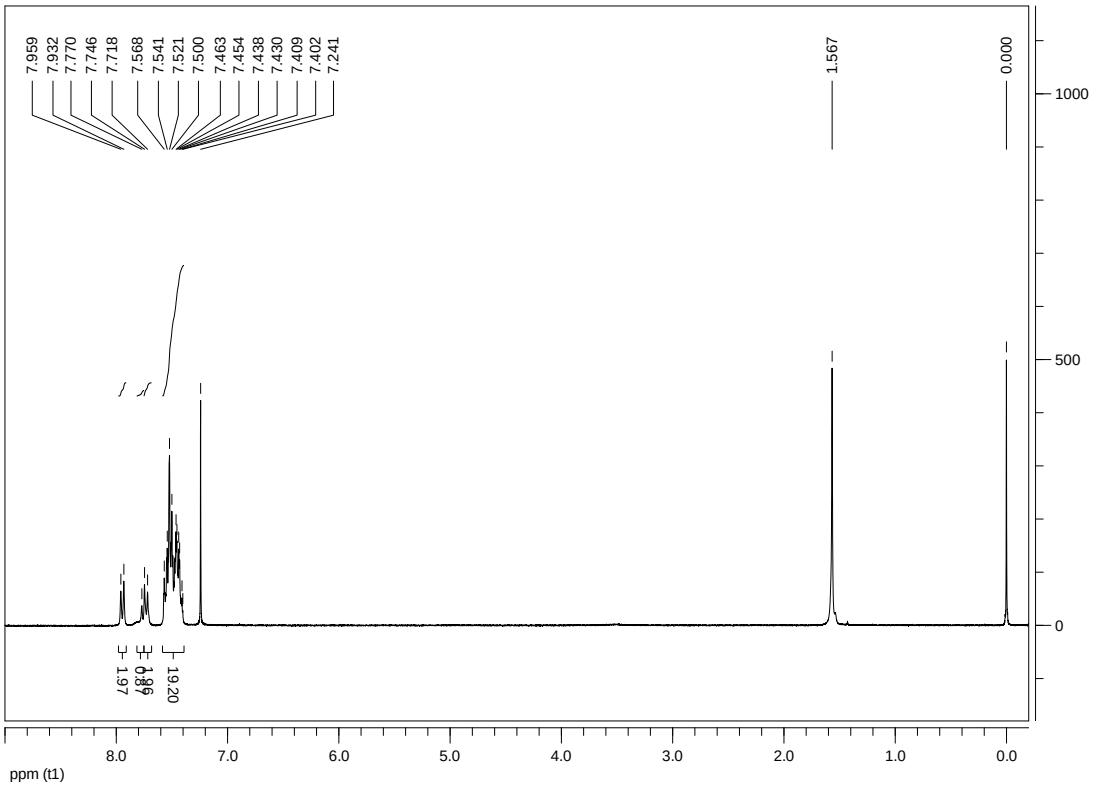

Figure S7. The ^{1}H NMR spectrum of **3b** in $CDCl_3$ at 298 K.

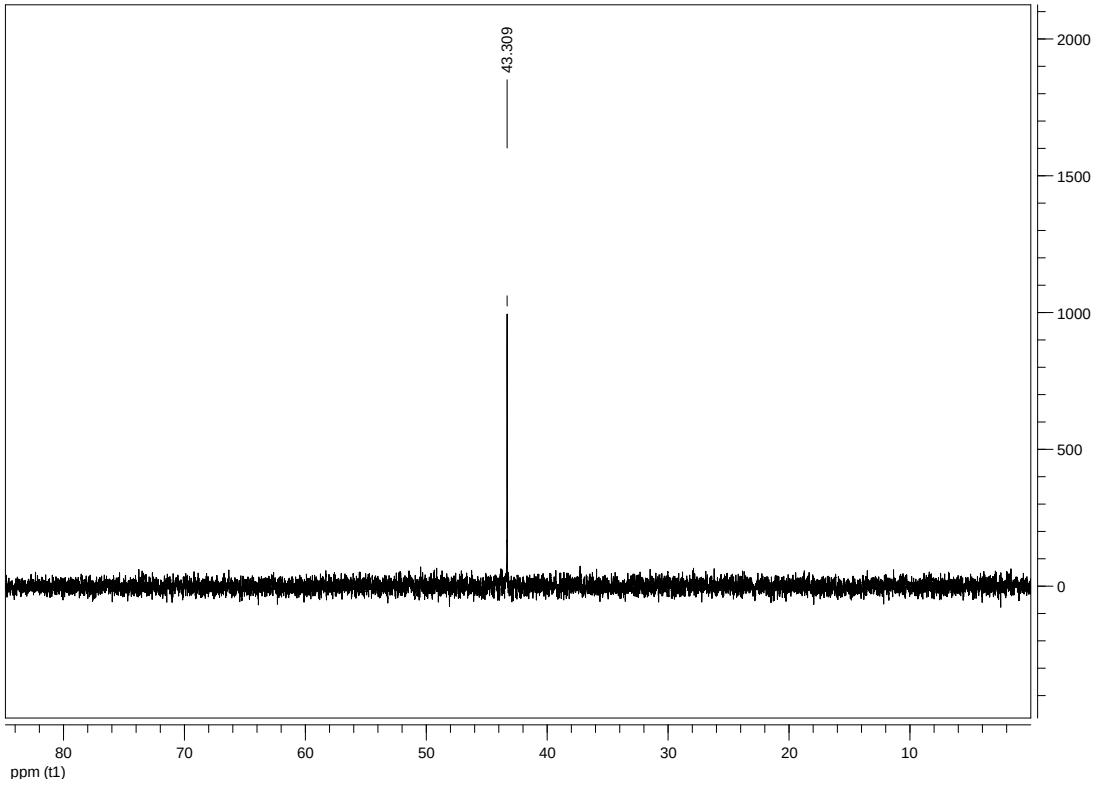

Figure S8. The ^{31}P NMR spectrum of **3b** in $CDCl_3$ at 298 K.

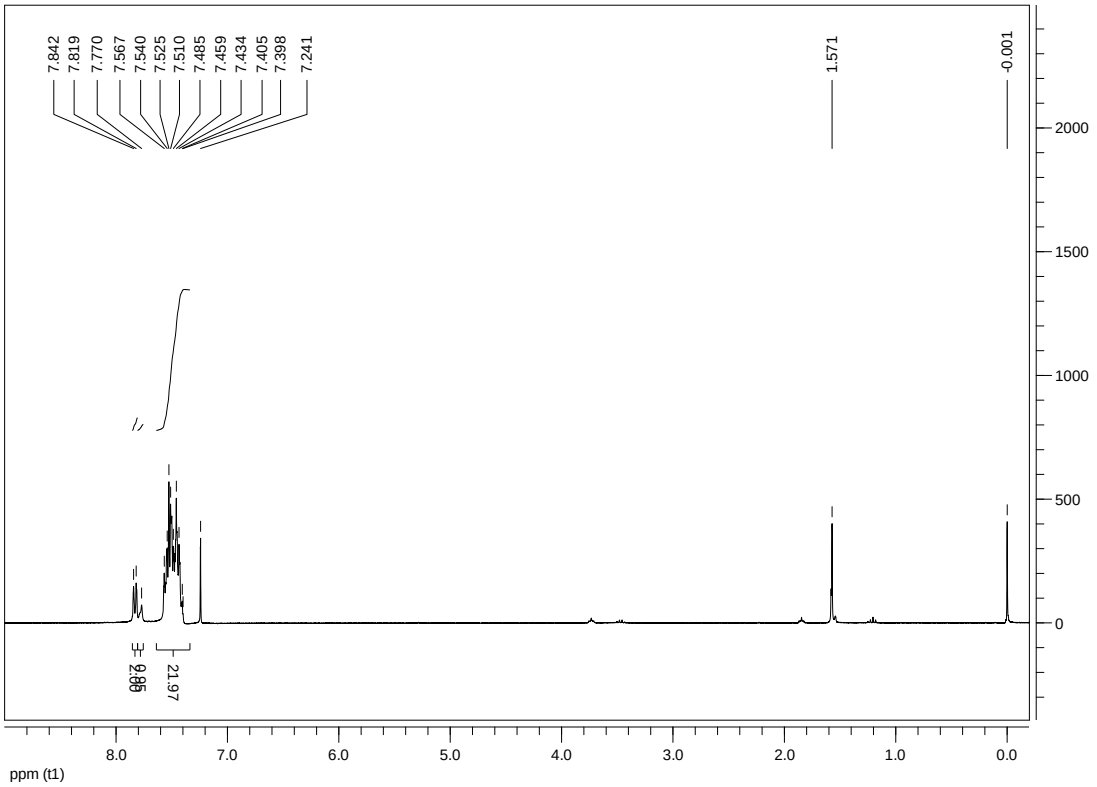

Figure S9. The ^{1}H NMR spectrum of **3c** in $CDCl_3$ at 298 K.

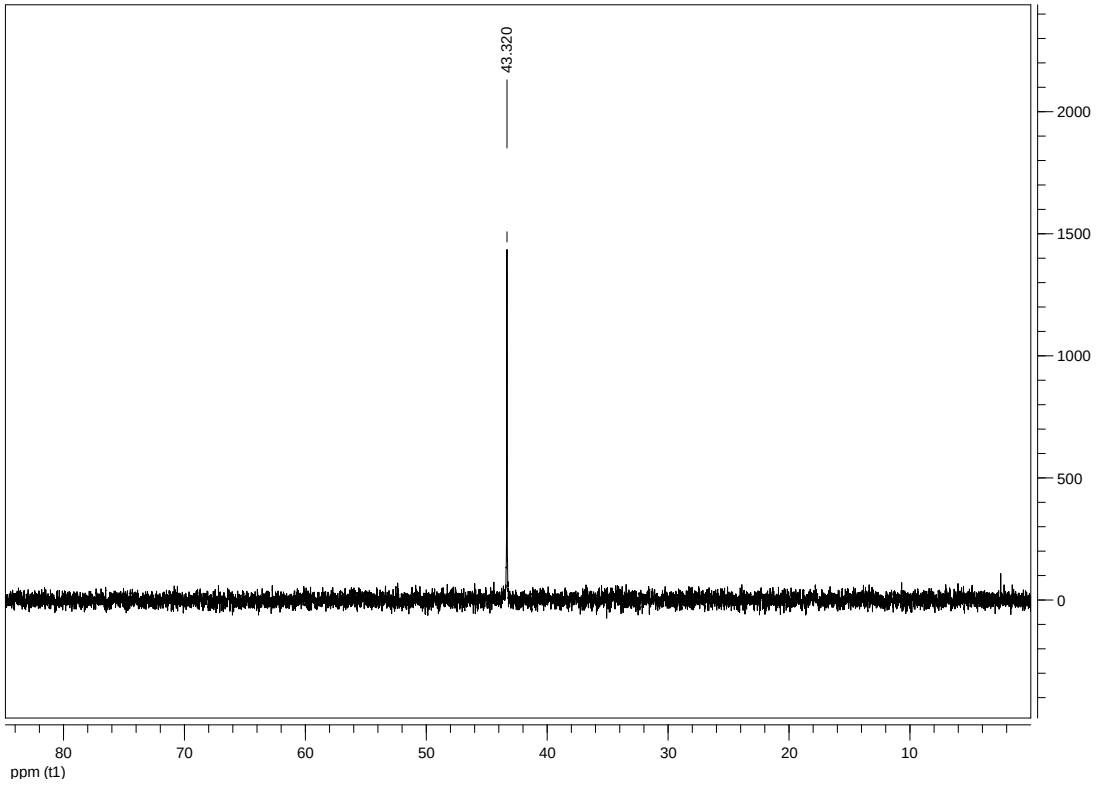

Figure S10. The ^{31}P NMR spectrum of **3c** in $CDCl_3$ at 298 K.

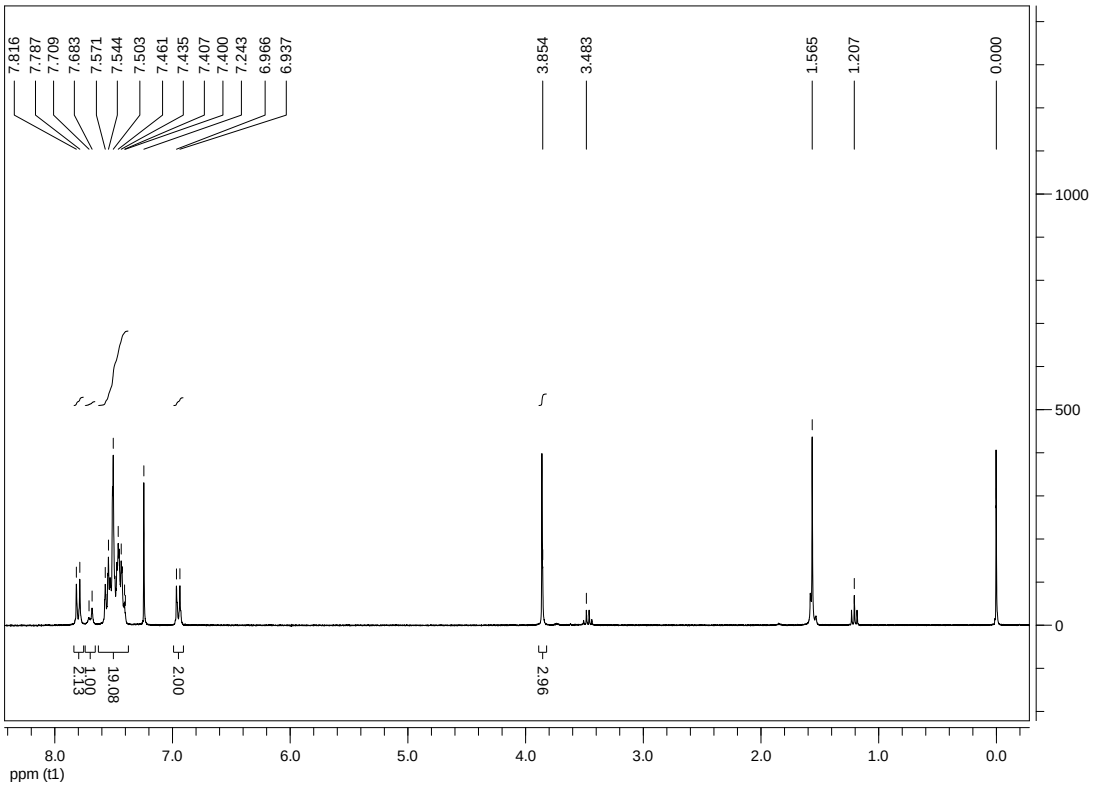

Figure S11. The ^{1}H NMR spectrum of **3d** in $CDCl_3$ at 298 K.

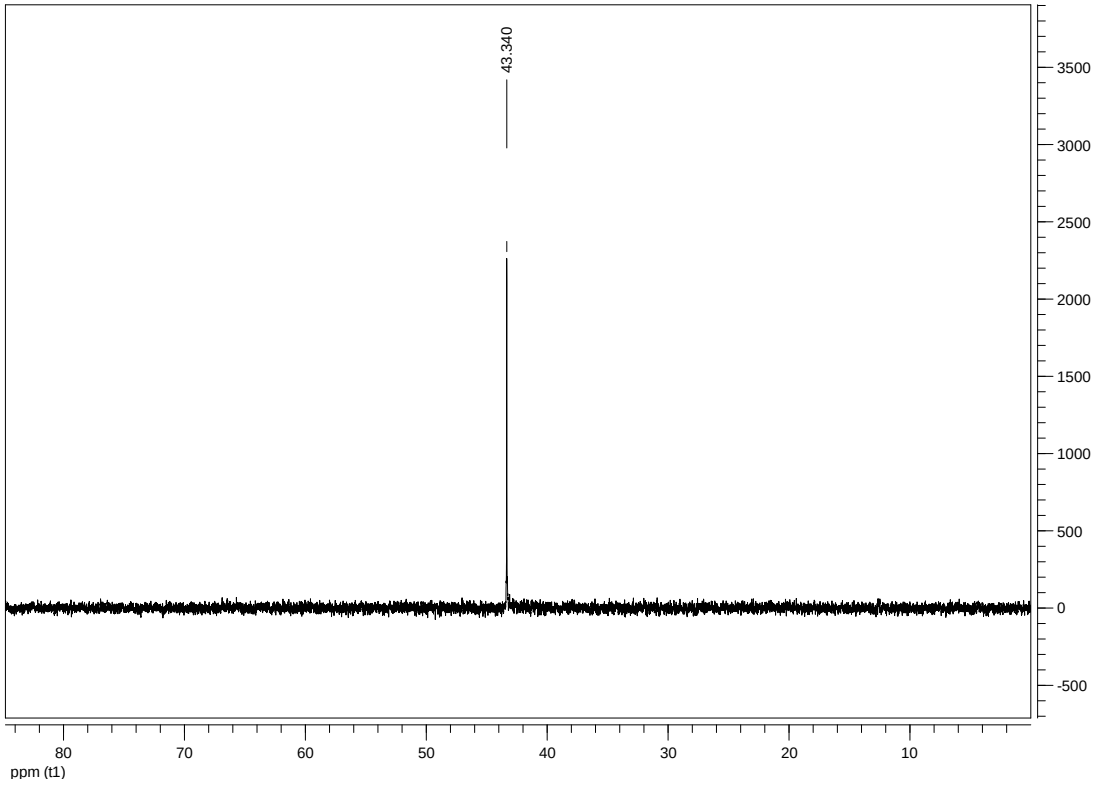

Figure S12. The ^{31}P NMR spectrum of **3d** in $CDCl_3$ at 298 K.

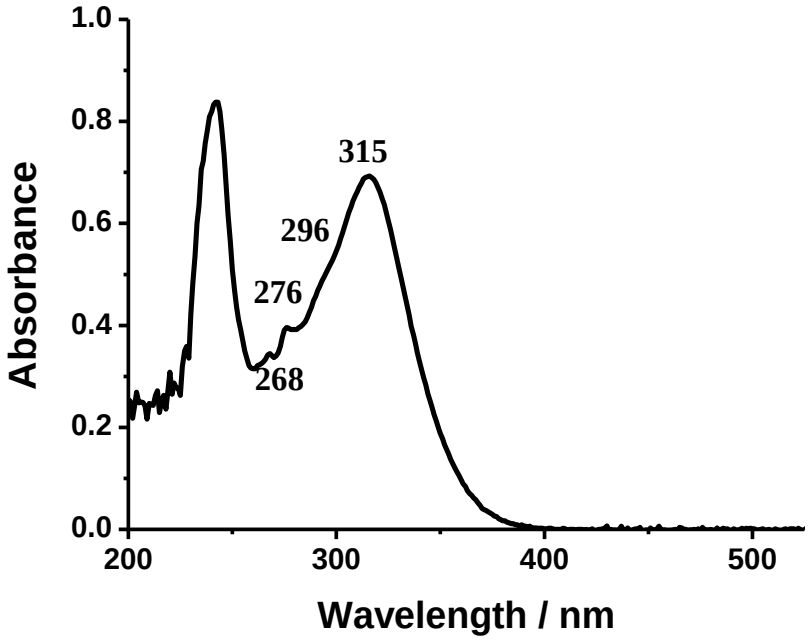

Figure S13. Electronic absorption spectrum of **3b** (1.98×10^{-5} mol dm^{-3}) in THF at 298 K.

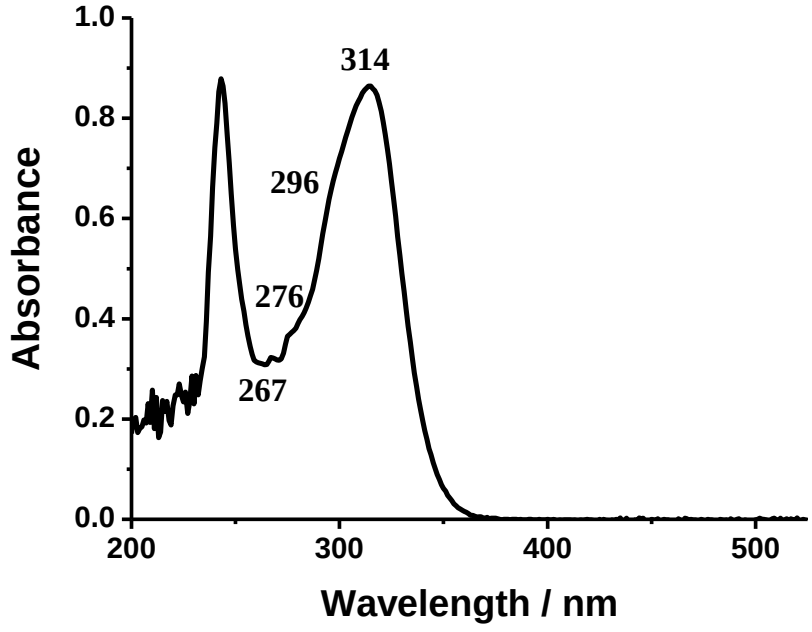

Figure S14. Electronic absorption spectrum of **3c** (1.98×10^{-5} mol dm^{-3}) in THF at 298 K.

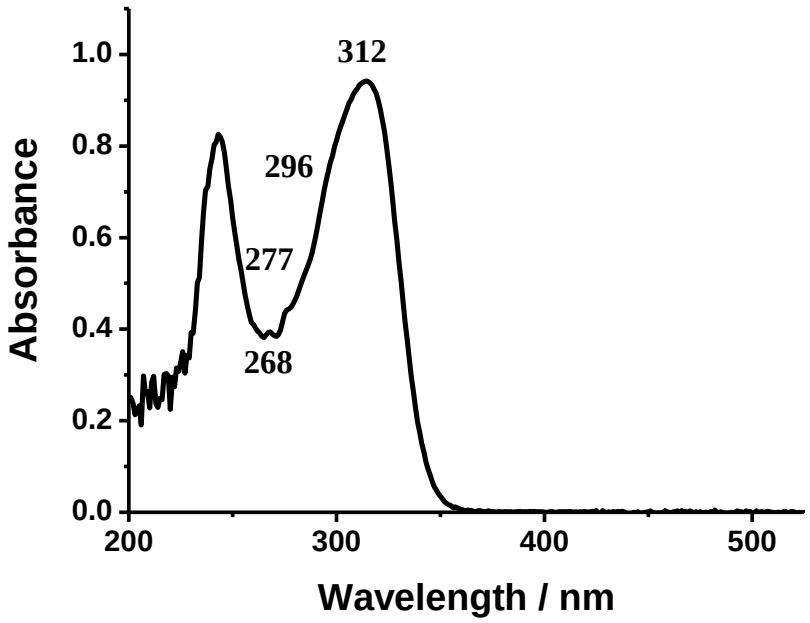

Figure S15. Electronic absorption spectrum of **3d** (1.98×10^{-5} mol dm^{-3}) in THF at 298 K.

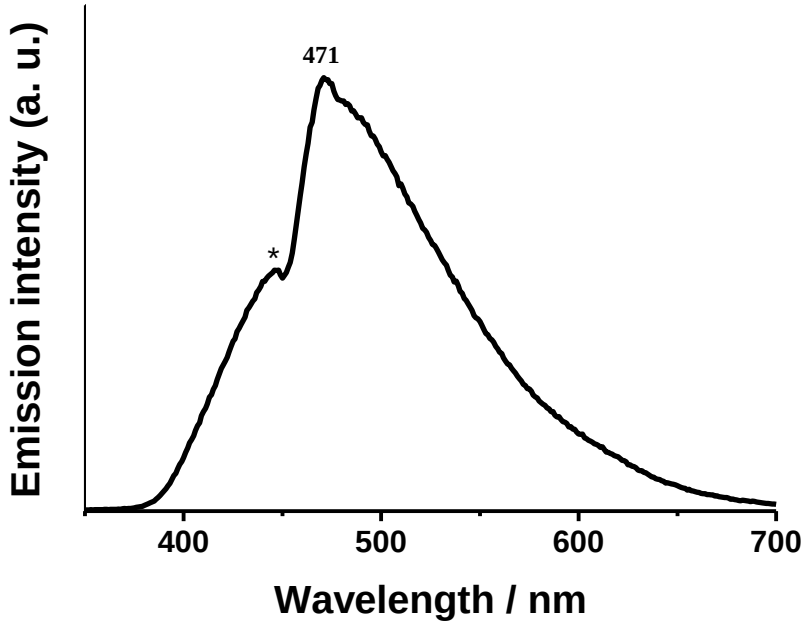

Figure S16. Emission spectrum of **3b** in the solid state at 298 K (λ_{ex} = 330 nm).

* denotes the artificial peak from the instrument

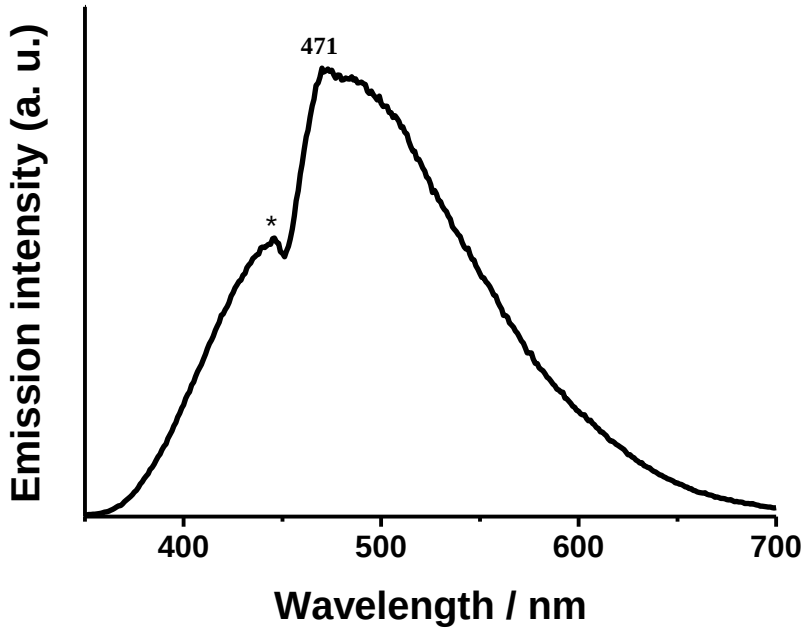

Figure S17. Emission spectrum of **3c** in the solid state at 298 K (λ_{ex}= 315 nm).

* denotes the artificial peak from the instrument

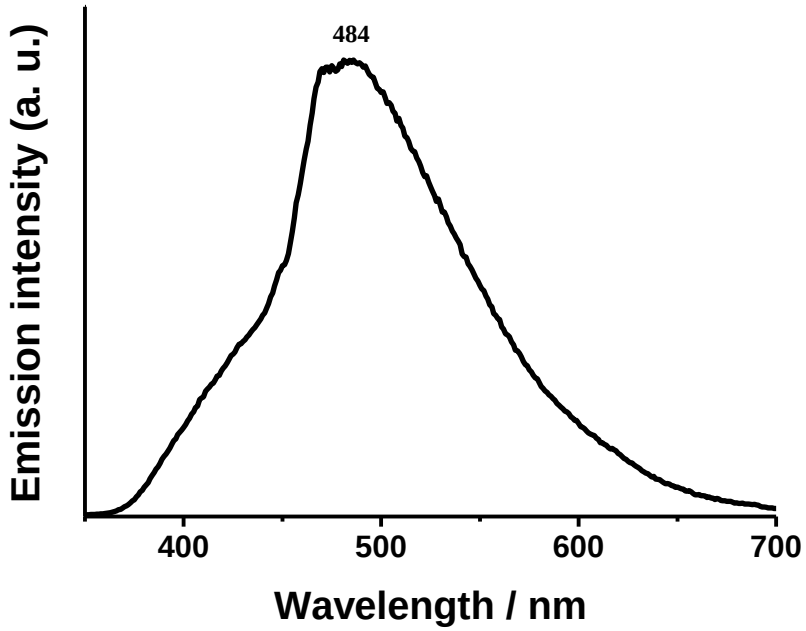

Figure S18. Emission spectrum of **3d** in the solid state at 298 K (λ_{ex} = 315 nm).

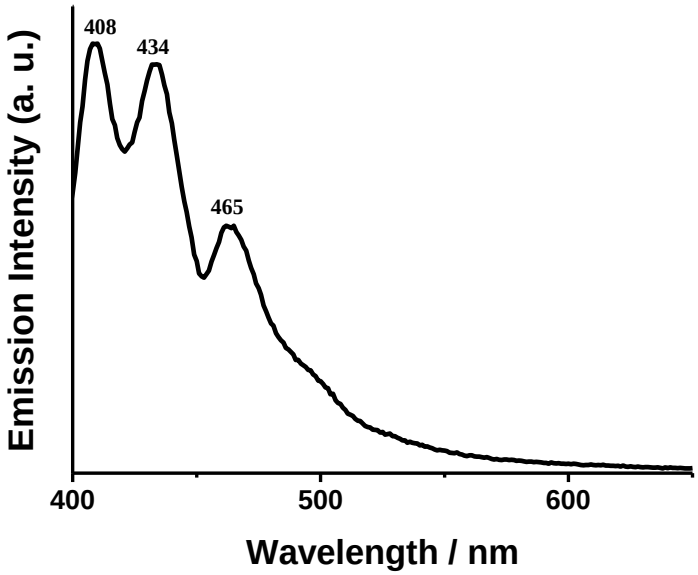

Figure S19. Emission spectrum of **3a** (1.98×10^{-5} mol dm^{-3}) in THF at 298 K (λ_{ex} = 330 nm).

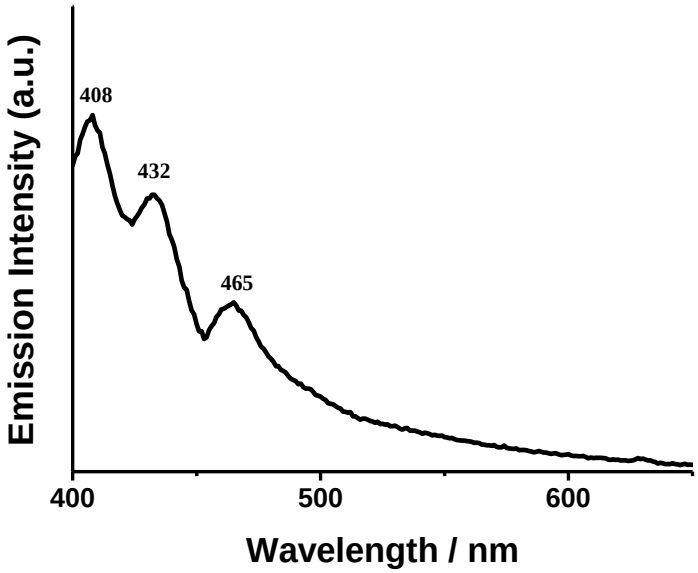

Figure S20. Emission spectroscopy of **3b** (1.98×10^{-5} mol dm^{-3}) in THF at 298 K (λ_{ex} = 315 nm).

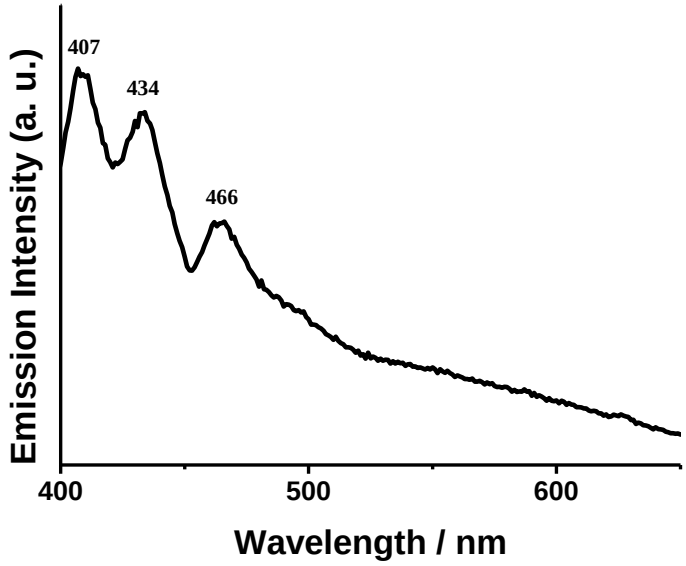

FigureS21. Emission spectrum of **3c** (1.98×10^{-5} mol dm^{-3}) in THF at 298 K (λ_{ex}= 315 nm).

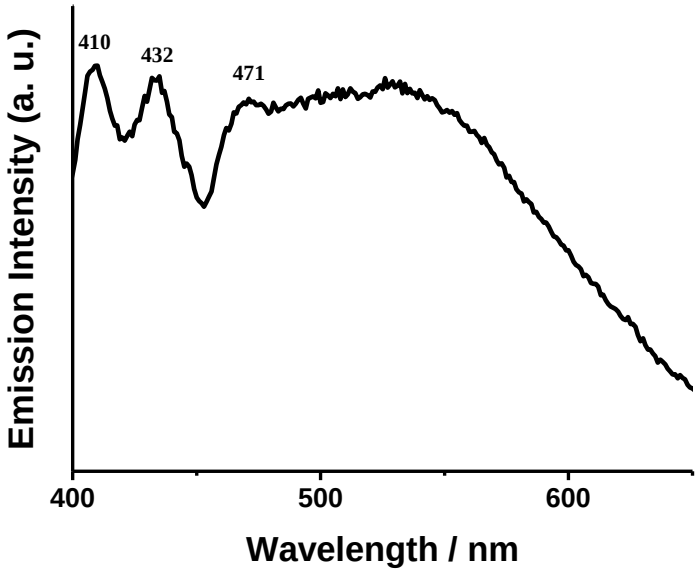

FigureS22. Emission spectrum of **3d** (1.98×10^{-5} mol dm^{-3}) in THF at 298 K (λ_{ex} = 315 nm).

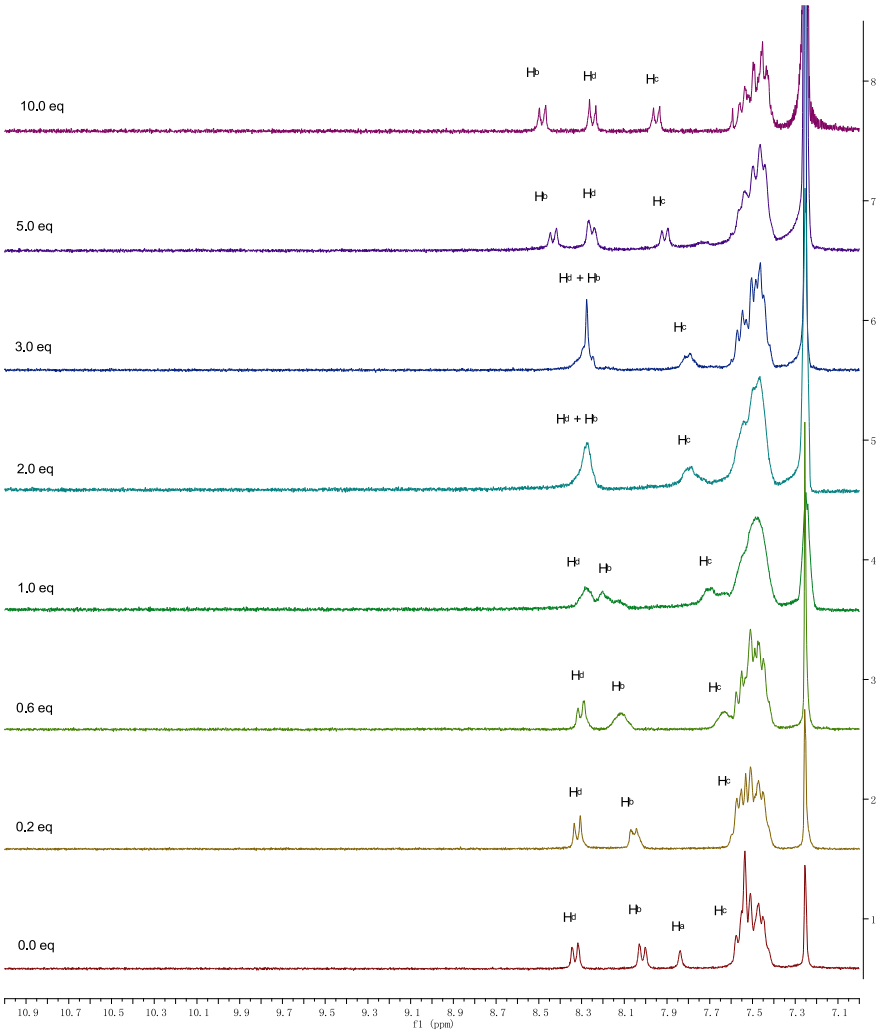

Figure S23. The ^{1}H NMR spectral changes of **3a** upon addition of F^{-} in $CDCl_3$ at 298 K.

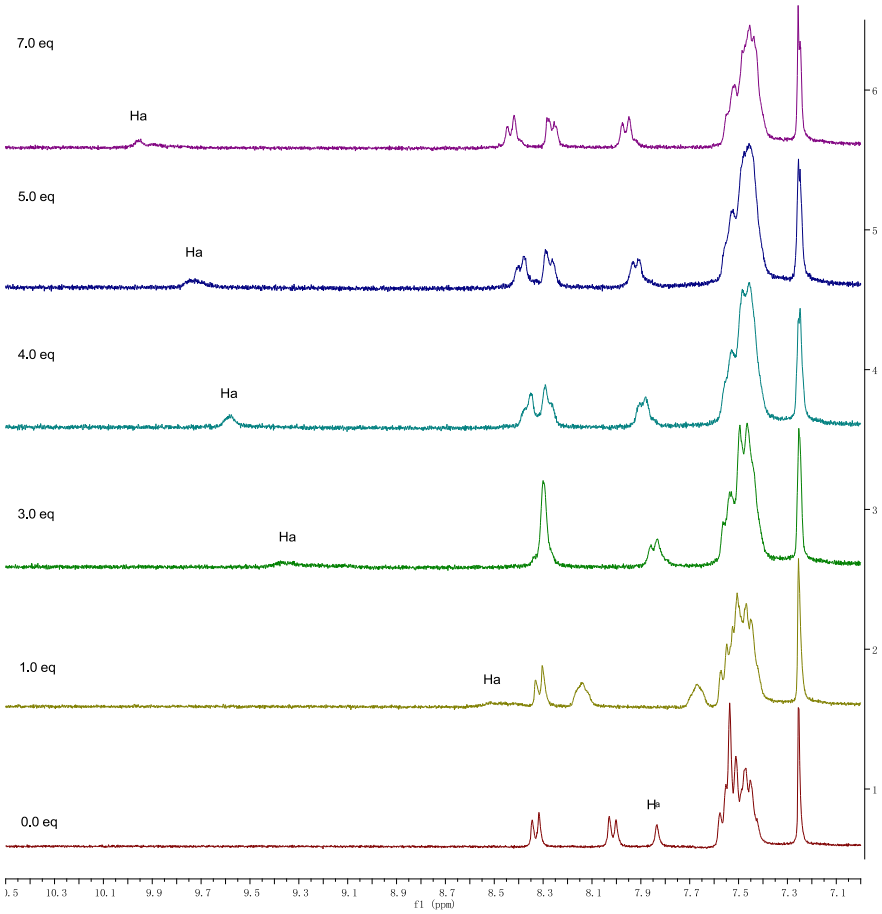

Figure S24. The ^{1}H NMR spectral changes of **3a** upon addition of Br^{-} in $CDCl_3$ at 298 K.

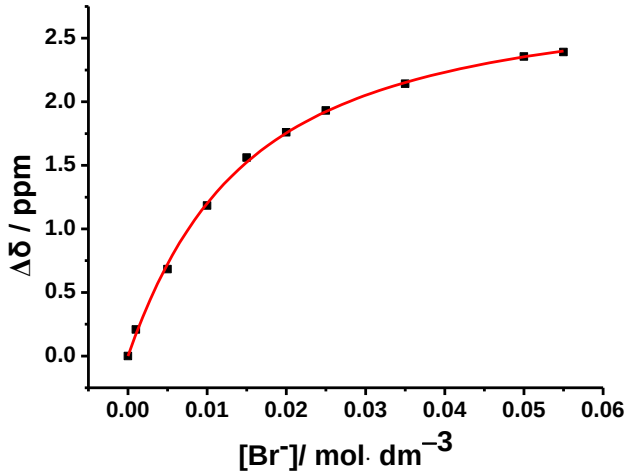

Figure S25. A plot of the chemical shift change of amide proton H_a as a function of [Br^{-}] and its theoretical fit for the 1:1 binding of **3a** with Br^{-}.

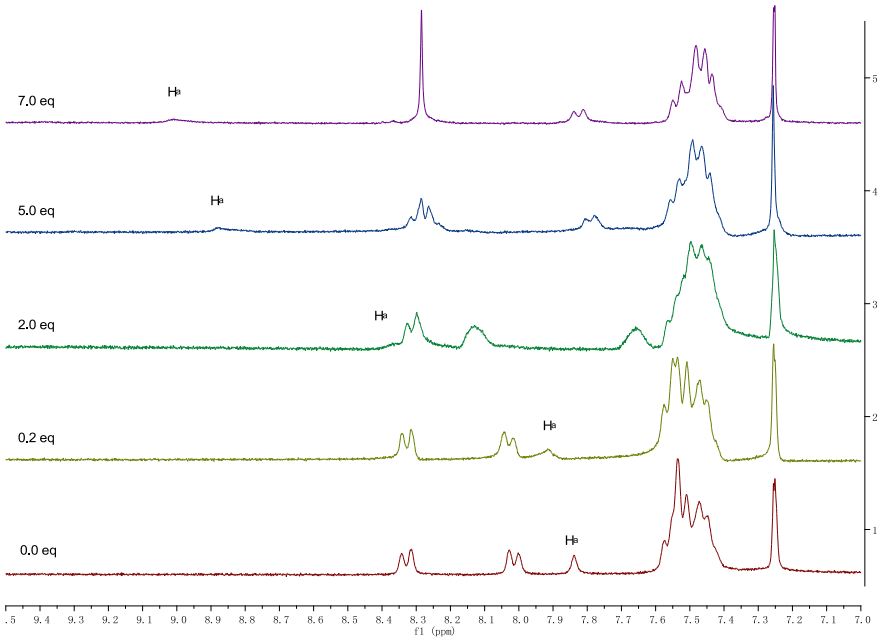

Figure S26. The ^{1}H NMR spectral changes of **3a** upon addition of I^- in $CDCl_3$ at 298 K.

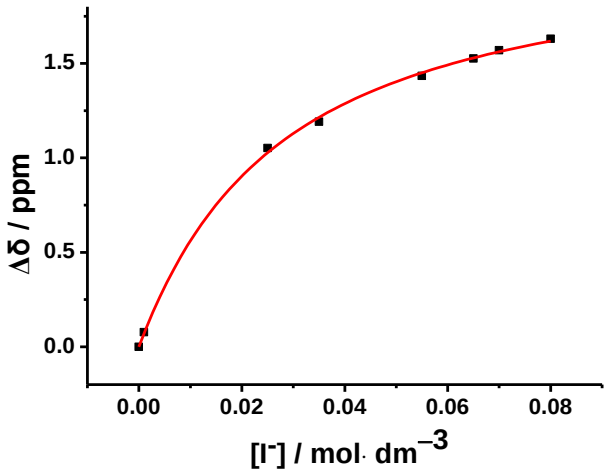

Figure S27. A plot of the chemical shift change of amide proton H_a as a function of [I^-] and its theoretical fit for the 1:1 binding of **3a** with I^-.

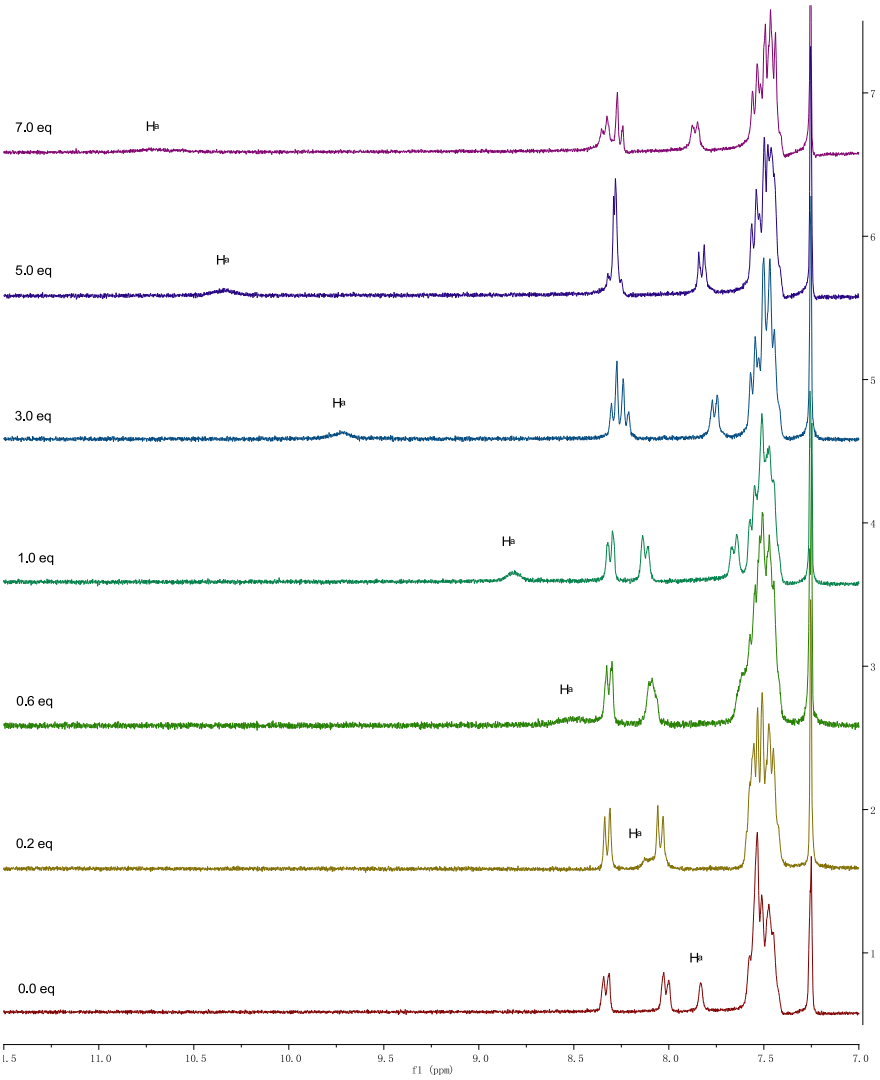

Figure S28. The ^{1}H NMR spectral changes of **3a** upon addition of OAc^{-} in $CDCl_3$ at 298 K.

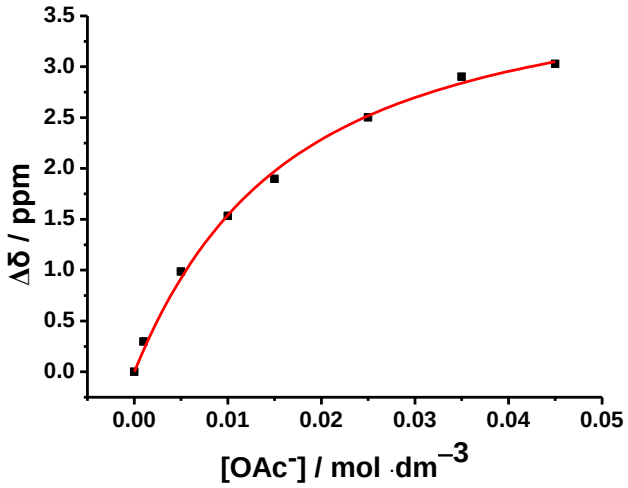

Figure S29. A plot of the chemical shift change of amide proton H_a as a function of [AcO^{-}] and its theoretical fit for the 1:1 binding of **3a** with AcO^{-}.

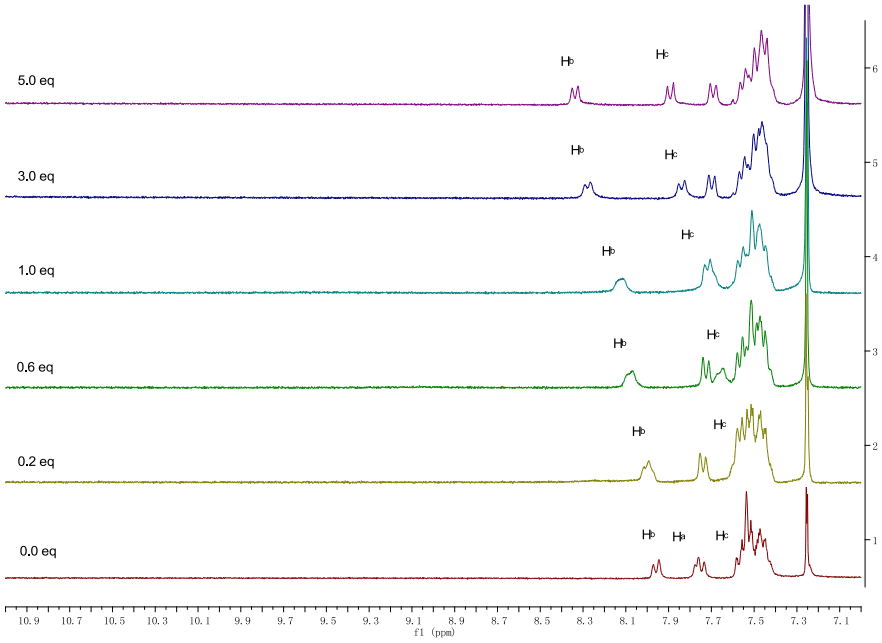

Figure S30. The ^{1}H NMR spectral changes of **3b** upon addition of F^{-} in $CDCl_3$ at 298 K.

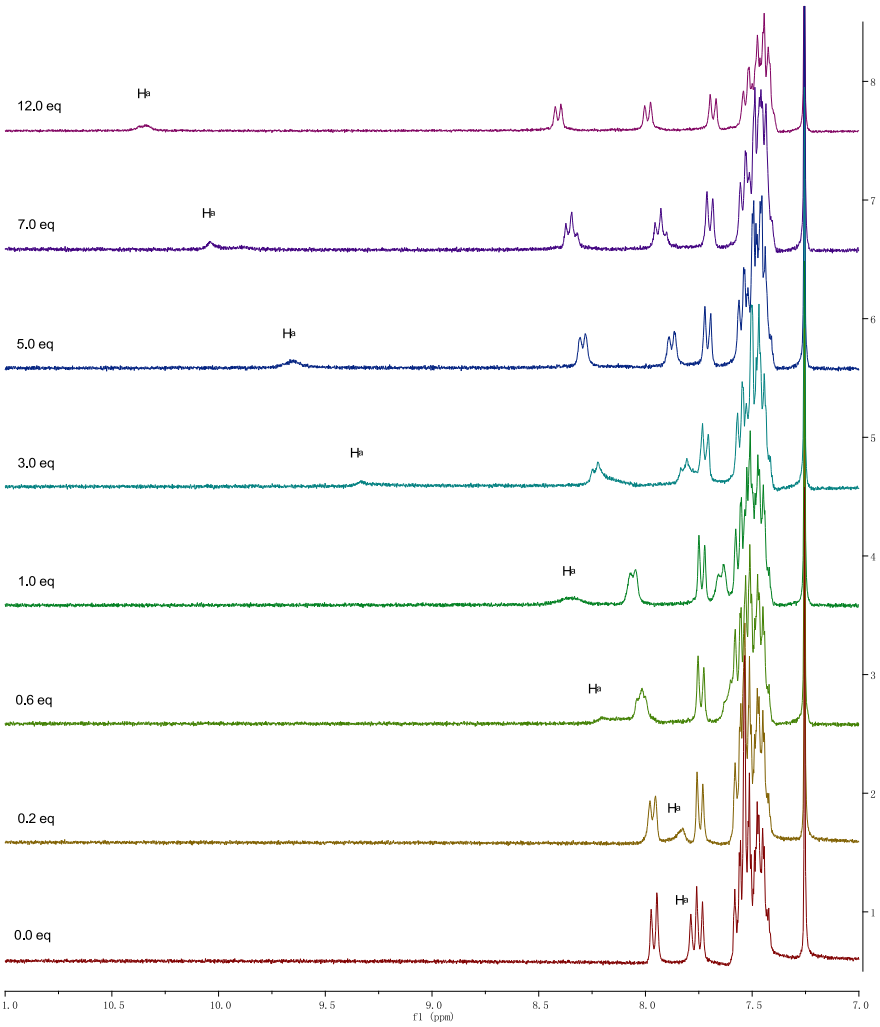

Figure S31. The ^{1}H NMR spectral changes of **3b** upon addition of Cl^- in $CDCl_3$ at 298 K.

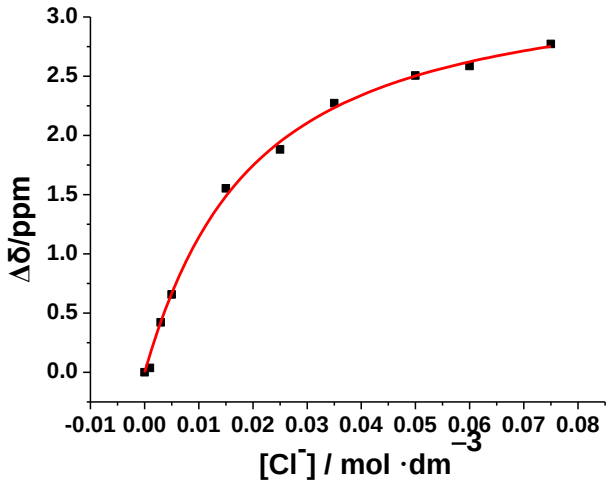

Figure S32. A plot of the chemical shift change of amide proton H_a as a function of [Cl^-] and its theoretical fit for the 1:1 binding of **3b** with Cl^-.

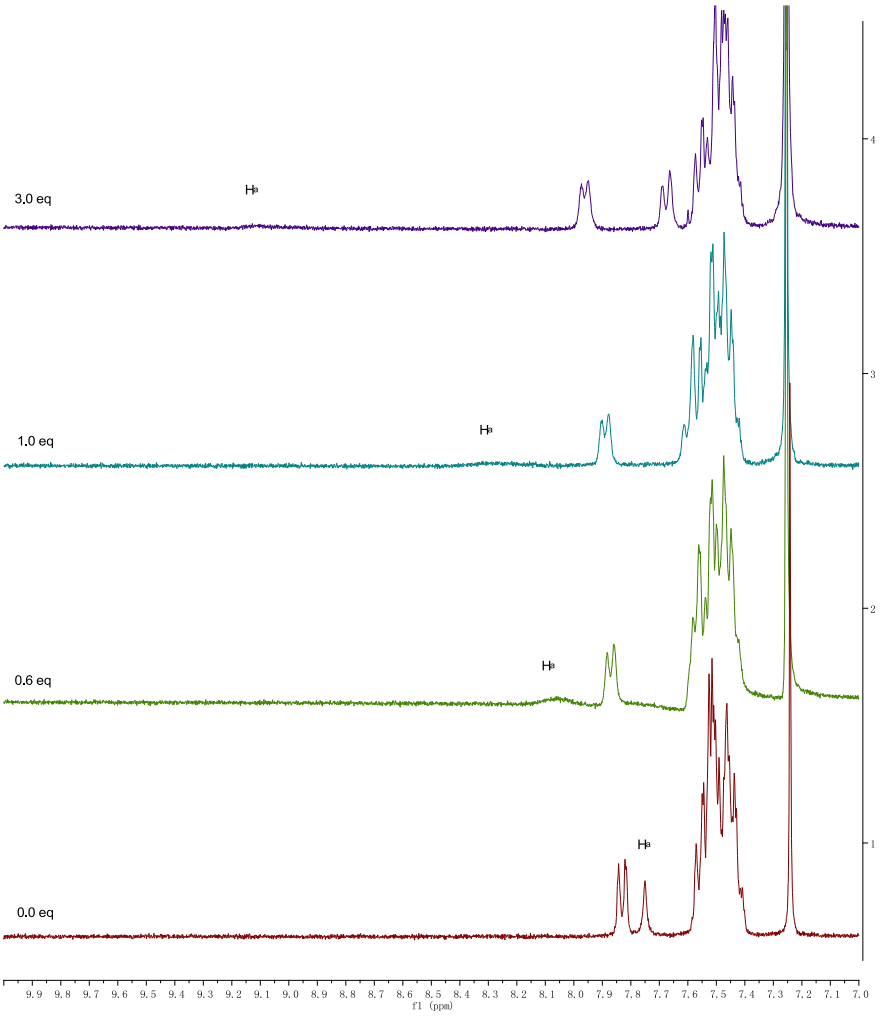

Figure S33. The ^{1}H NMR spectral changes of **3c** upon addition of F^- in $CDCl_3$ at 298 K.

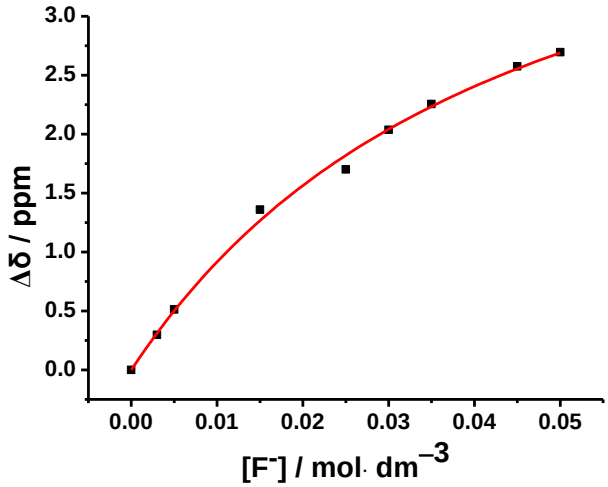

Figure S34. A plot of the chemical shift change of amide proton H_a as a function of [F^-] and its theoretical fit for the 1:1 binding of **3c** with F^-.

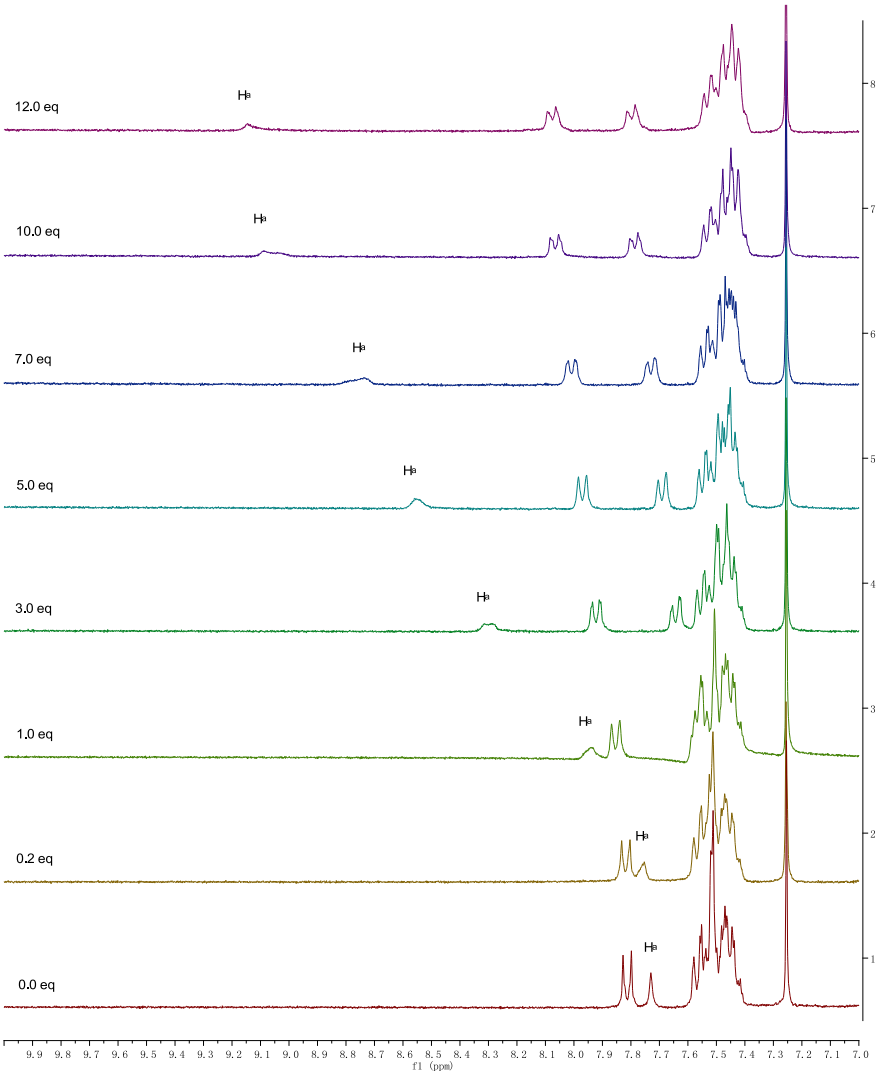

Figure S35. The ^{1}H NMR spectral changes of **3c** upon addition of Cl^- in $CDCl_3$ at 298 K.

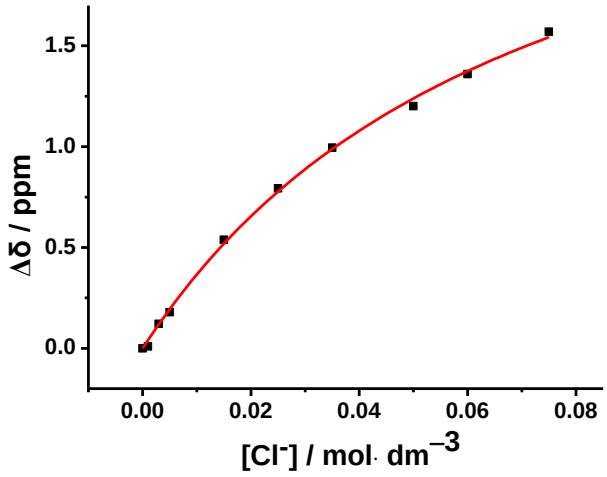

Figure S36. A plot of the chemical shift change of amide proton H_a as a function of [Cl^-] and its theoretical fit for the 1:1 binding of **3c** with Cl^-.

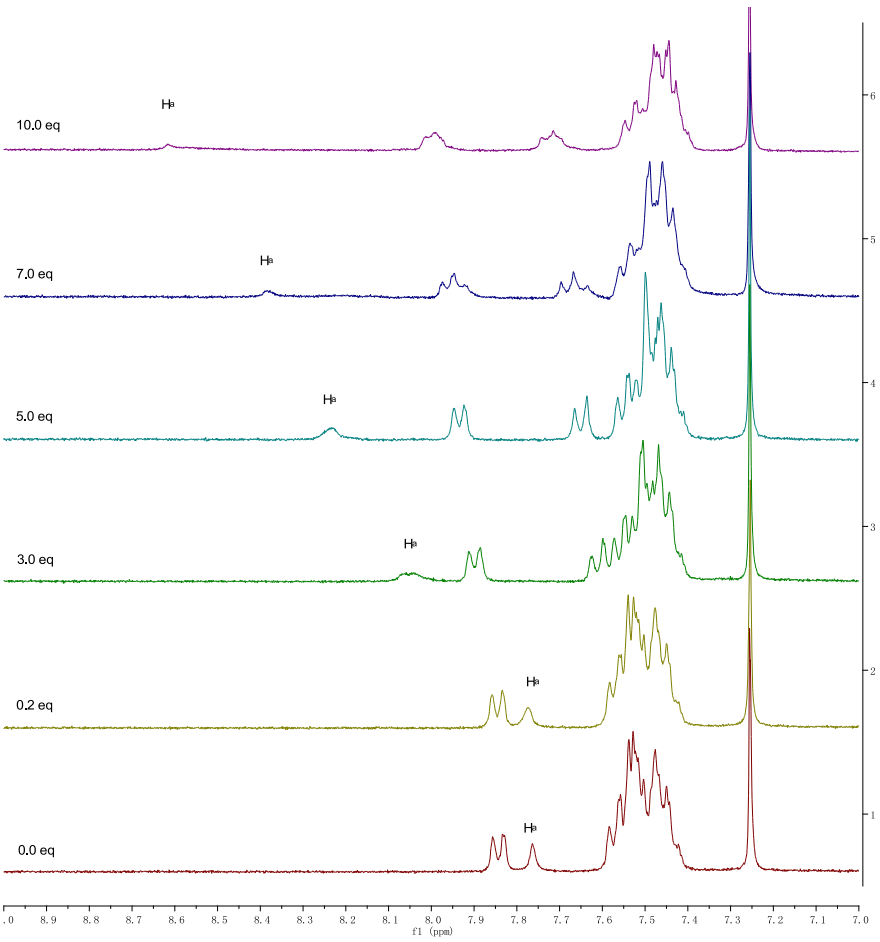

Figure S37. The ^{1}H NMR spectral changes of **3c** upon addition of Br^{-} in $CDCl_3$ at 298 K.

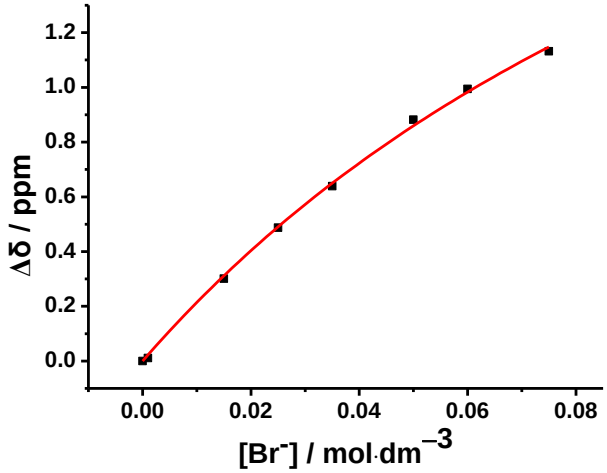

Figure S38. A plot of the chemical shift change of amide proton H_a as a function of [Br^{-}] and its theoretical fit for the 1:1 binding of **3c** with Br^{-}.

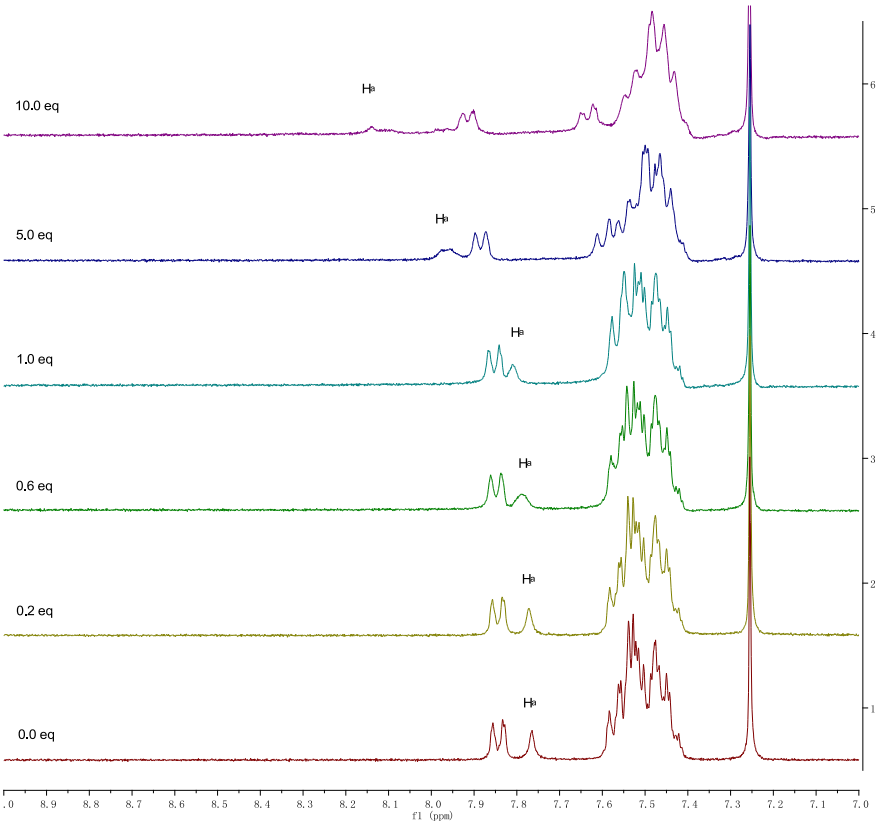

Figure S39. The ^{1}H NMR spectral changes of **3c** upon addition of I^- in $CDCl_3$ at 298 K.

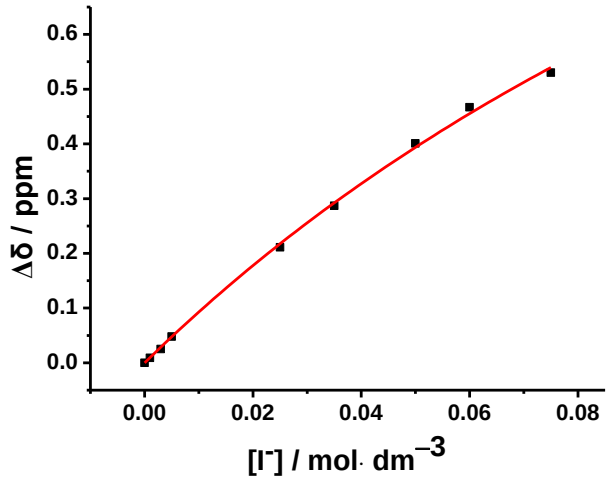

Figure S40. A plot of the chemical shift change of amide proton H_a as a function of [I^-] and its theoretical fit for the 1:1 binding of **3c** with I^-.

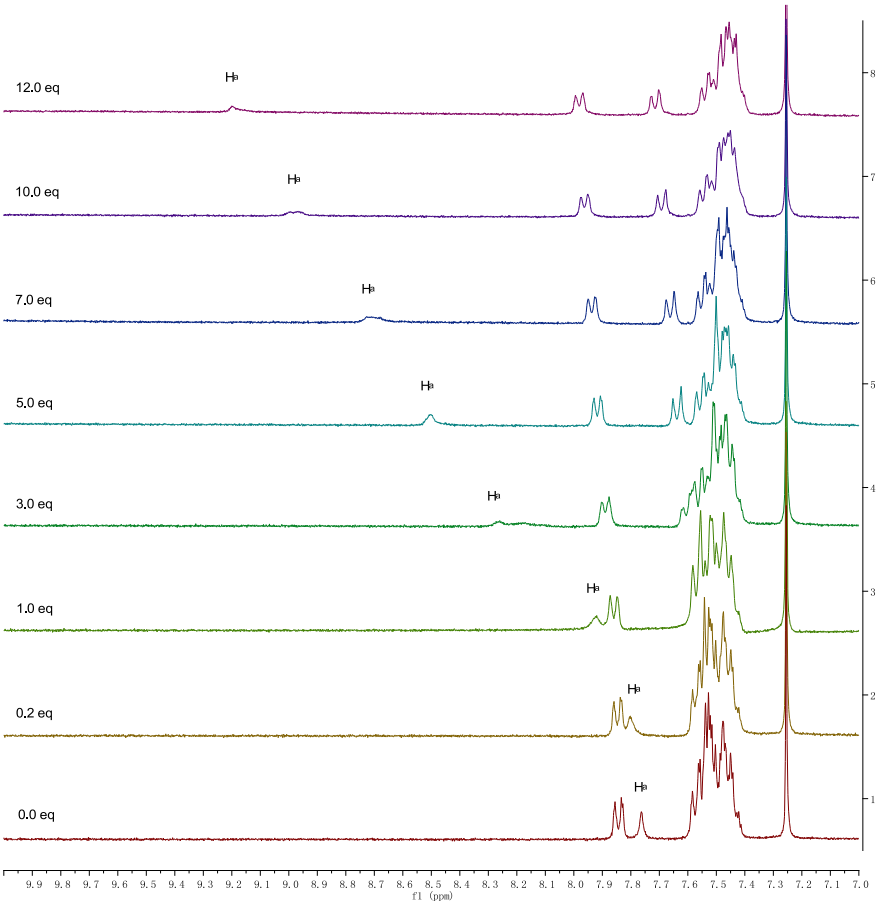

Figure S41. The ^{1}H NMR spectral changes of **3c** upon addition of OAc^- in $CDCl_3$ at 298 K.

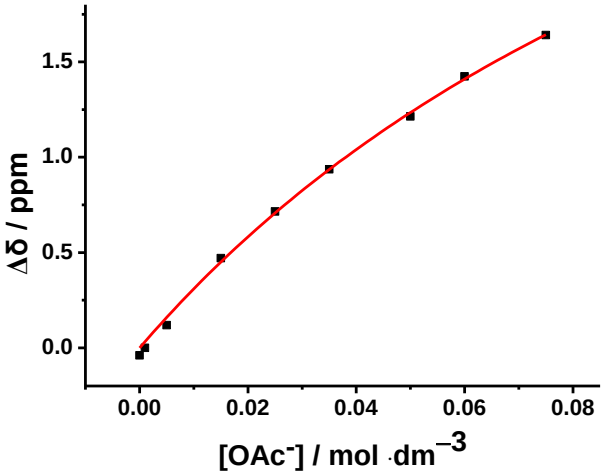

Figure S42. A plot of the chemical shift change of amide proton H_a as a function of [AcO^-] and its theoretical fit for the 1:1 binding of **3c** with AcO^-.

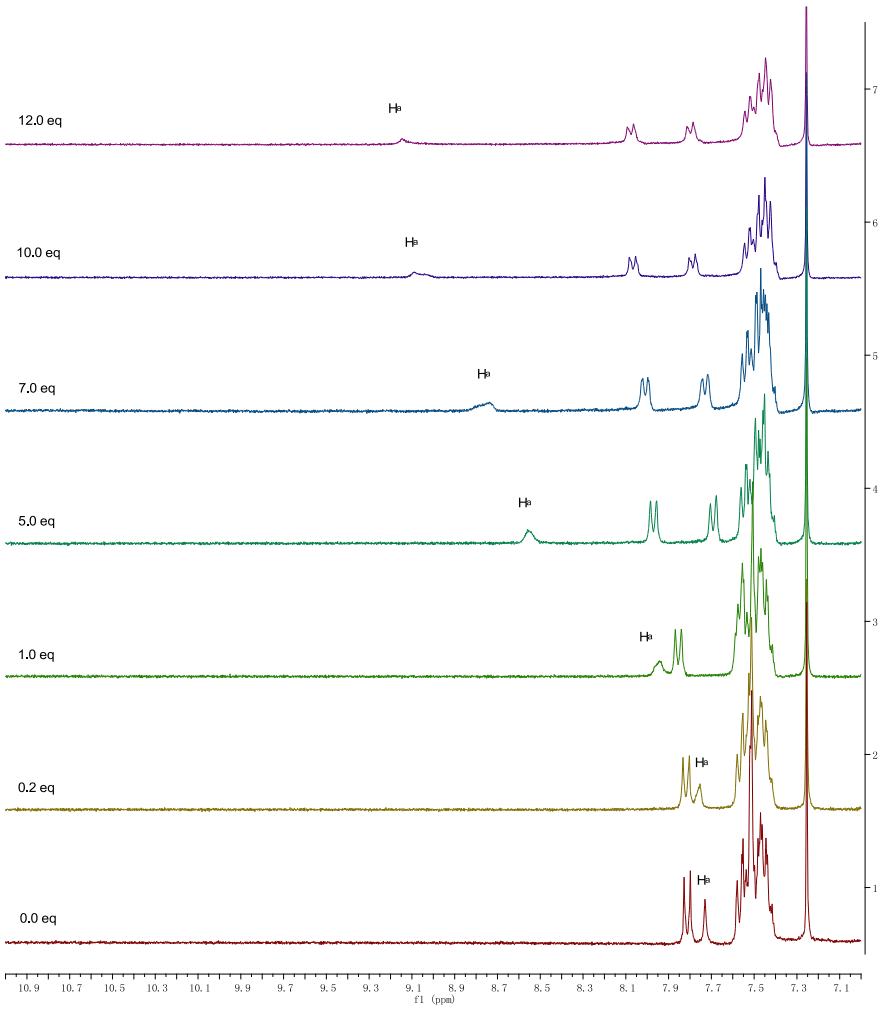

Figure S43. The ^{1}H NMR spectral changes of **3d** upon addition of Cl^{-} in $CDCl_3$ at 298 K.

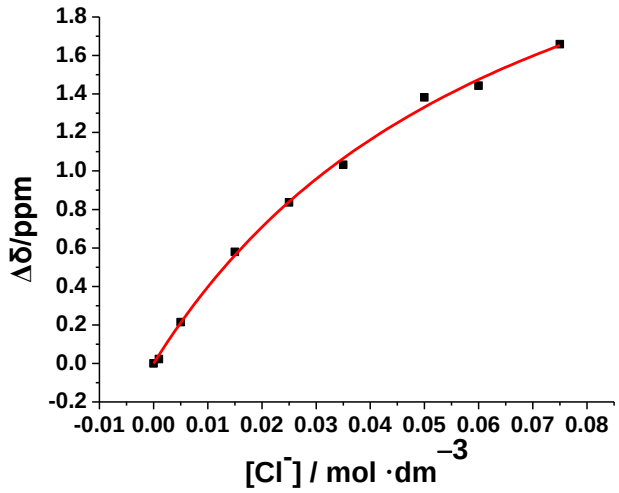

Figure S44. A plot of the chemical shift change of amide proton H_a as a function of [Cl^{-}] and its theoretical fit for the 1:1 binding of **3d** with Cl^{-}.

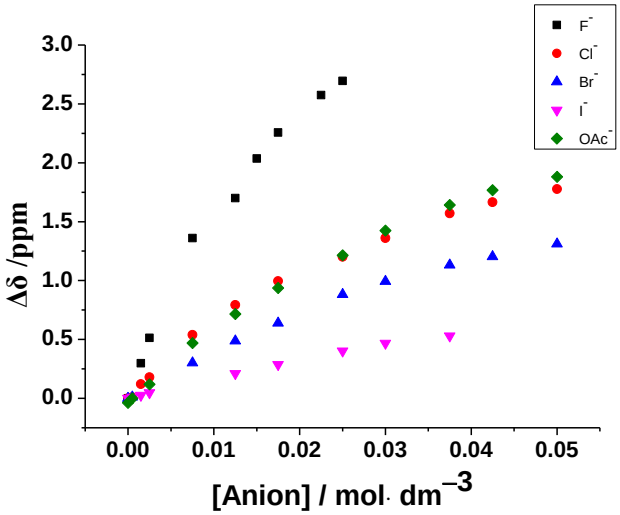

Figure S45. The shifts of the signals of amide N–H (H_a) of **3c** upon addition of different anions with different concentrations in $CDCl_3$ at 298 K.

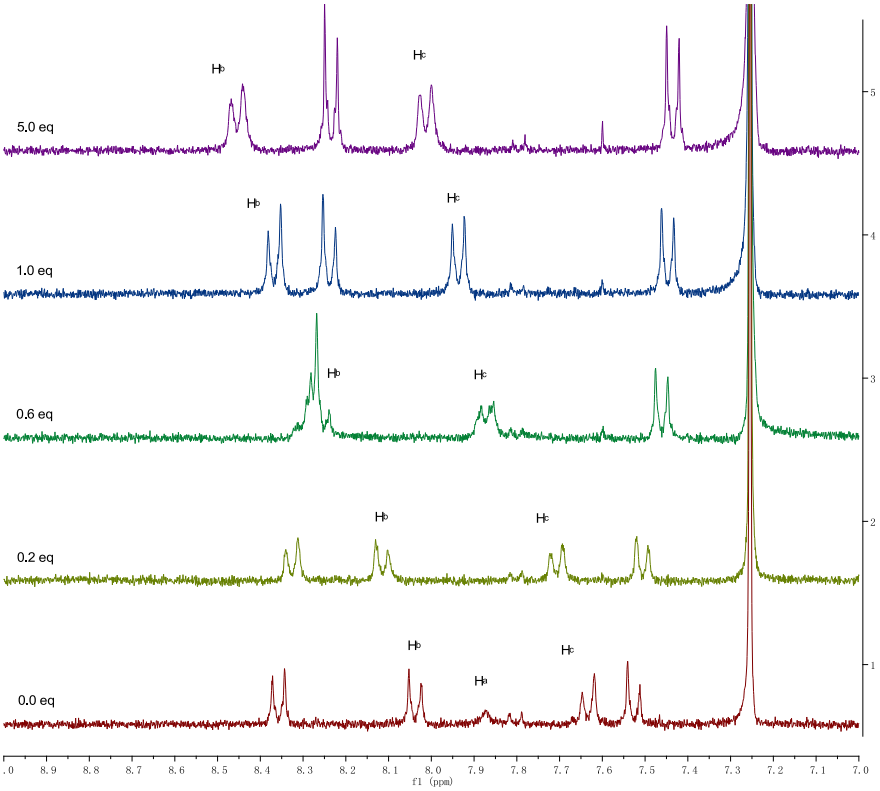

Figure S46. The ^1H NMR spectral changes of **4a** upon addition of F^- in $CDCl_3$ at 298 K.

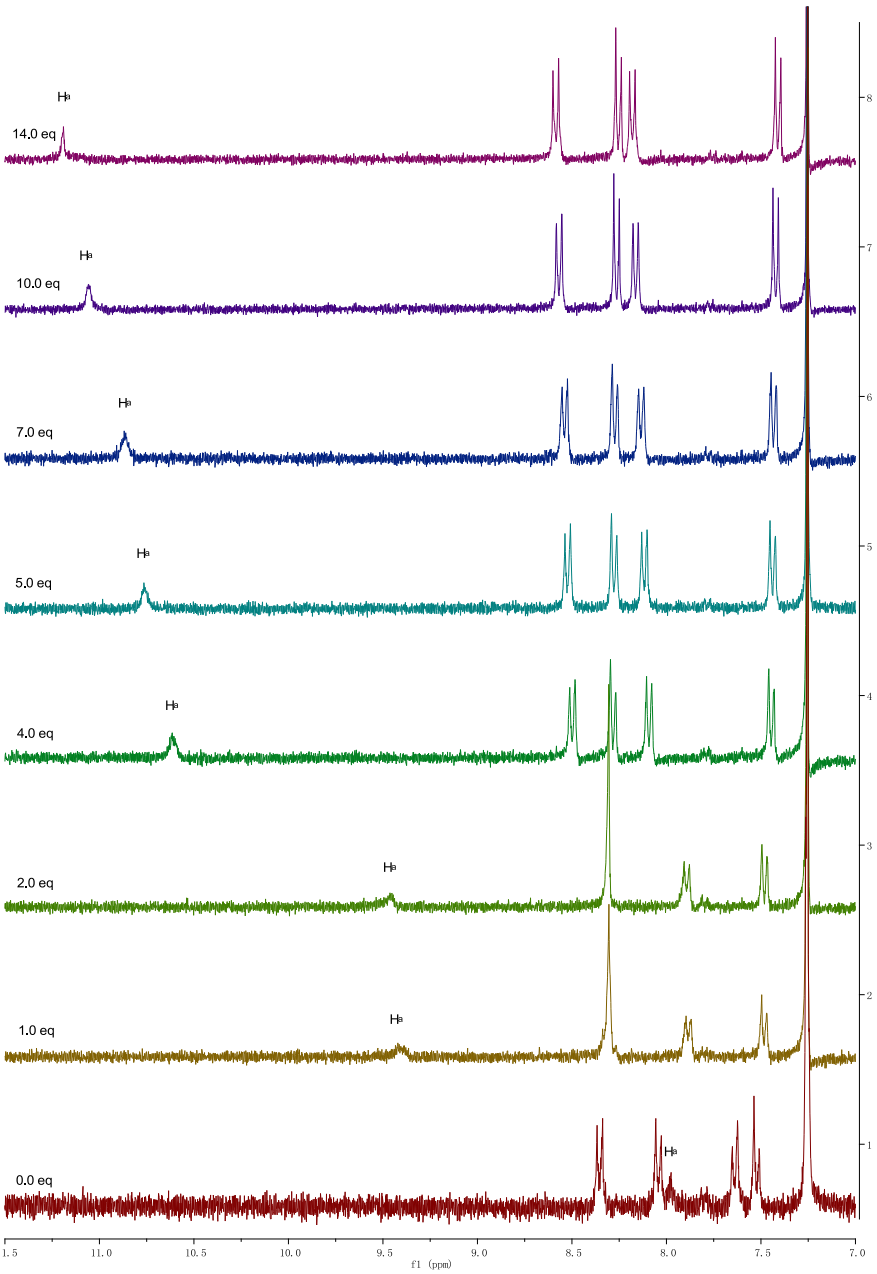

Figure S47. The ^{1}H NMR spectral changes of **4a** upon addition of Cl^{-} in $CDCl_3$ at 298 K.

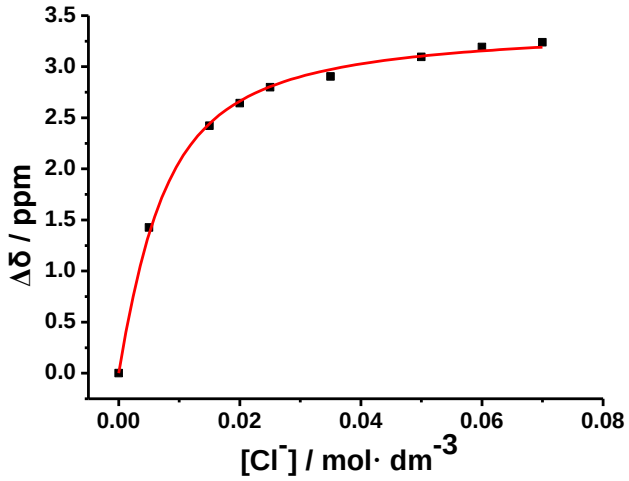

Figure S48. A plot of the chemical shift change of amide proton H_a as a function of [Cl^-] and its theoretical fit for the 1:1 binding of **4a** with Cl^-.

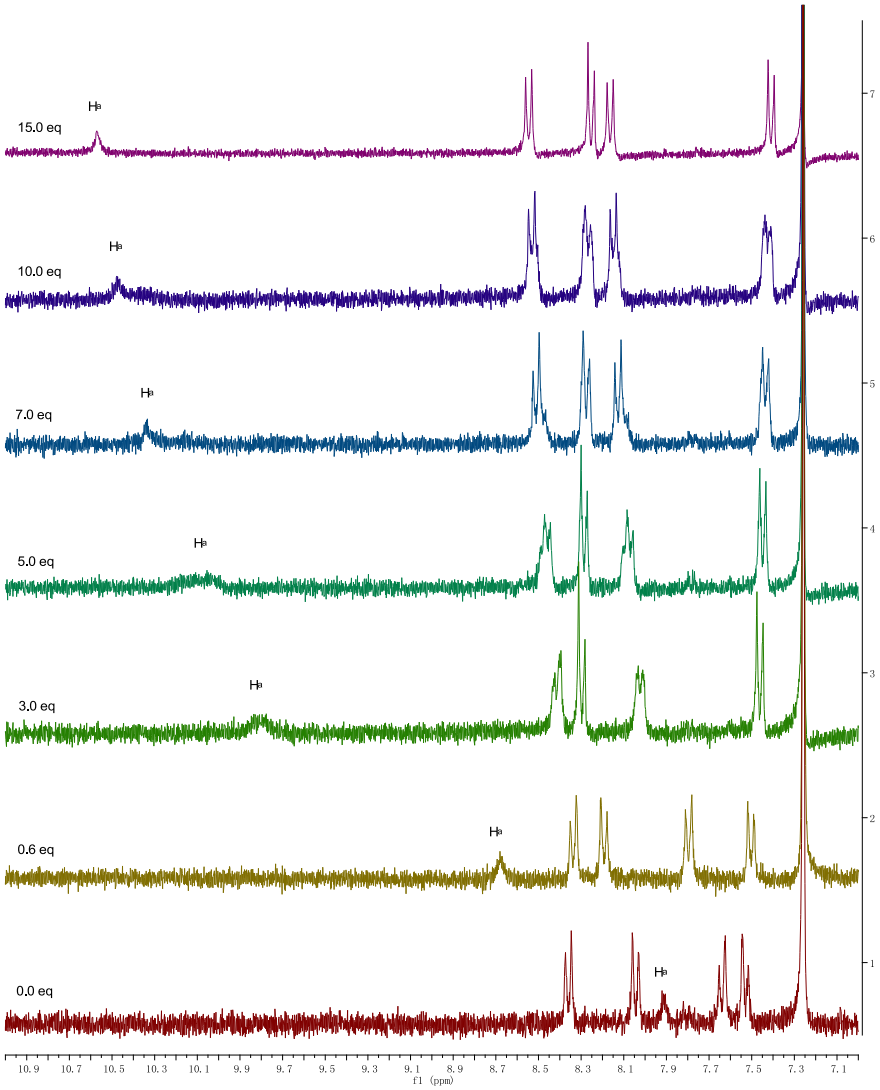

Figure S49. The ^{1}H NMR spectral changes of **4a** upon addition of Br^- in $CDCl_3$ at 298 K.

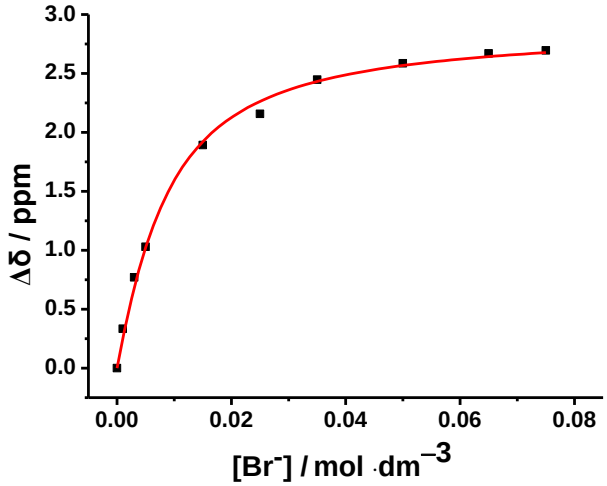

Figure S50. A plot of the chemical shift change of amide proton H_a as a function of [Br^-] and its theoretical fit for the 1:1 binding of **4a** with Br^-.

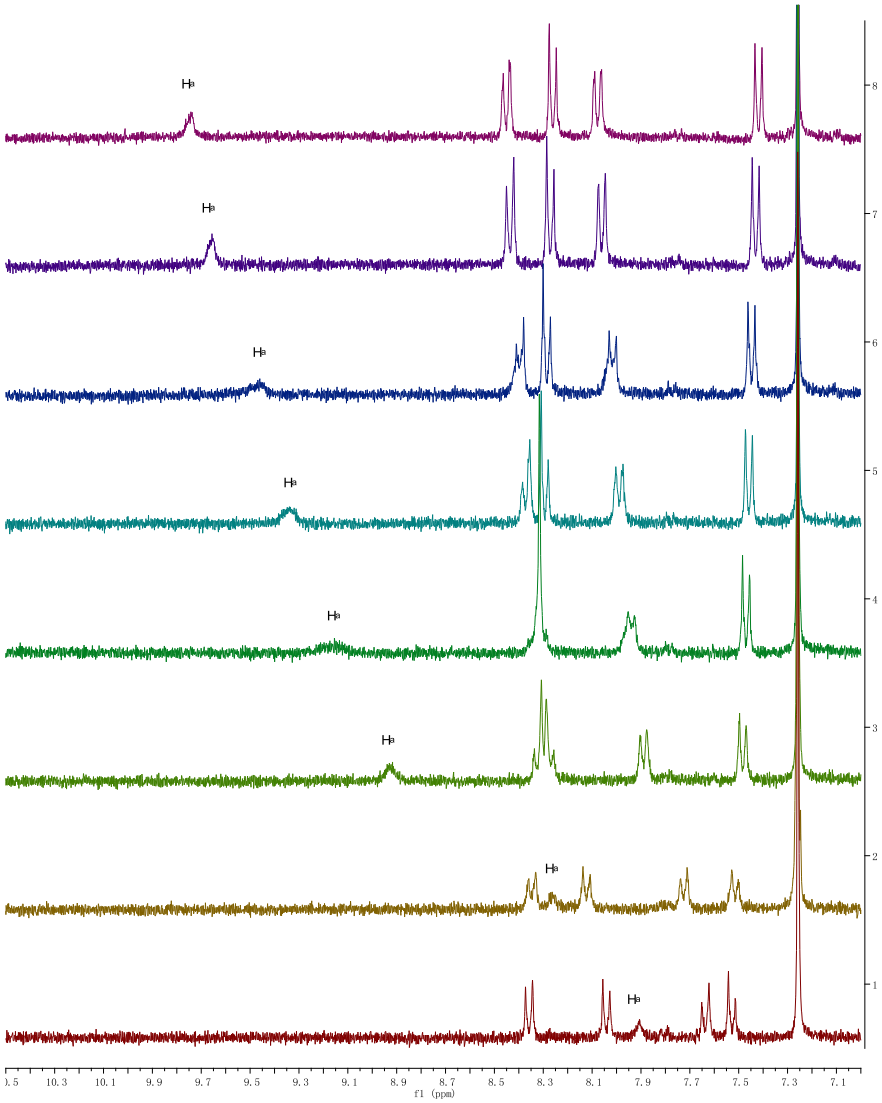

Figure S51. The ^{1}H NMR spectral changes of **4a** upon addition of I^- in $CDCl_3$ at 298 K.

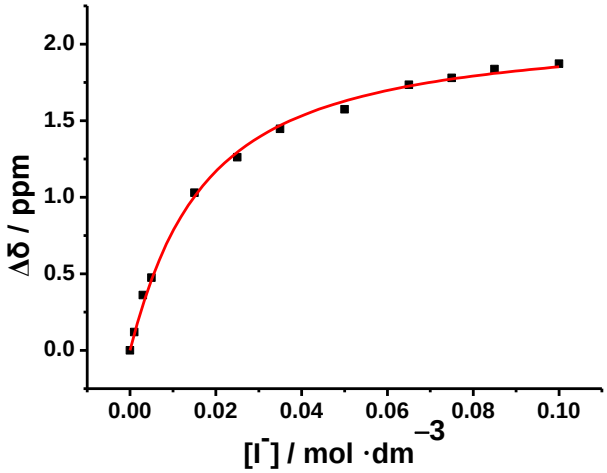

Figure S52. A plot of the chemical shift change of amide proton H_a as a function of [I^-] and its theoretical fit for the 1:1 binding of **4a** with I^-.

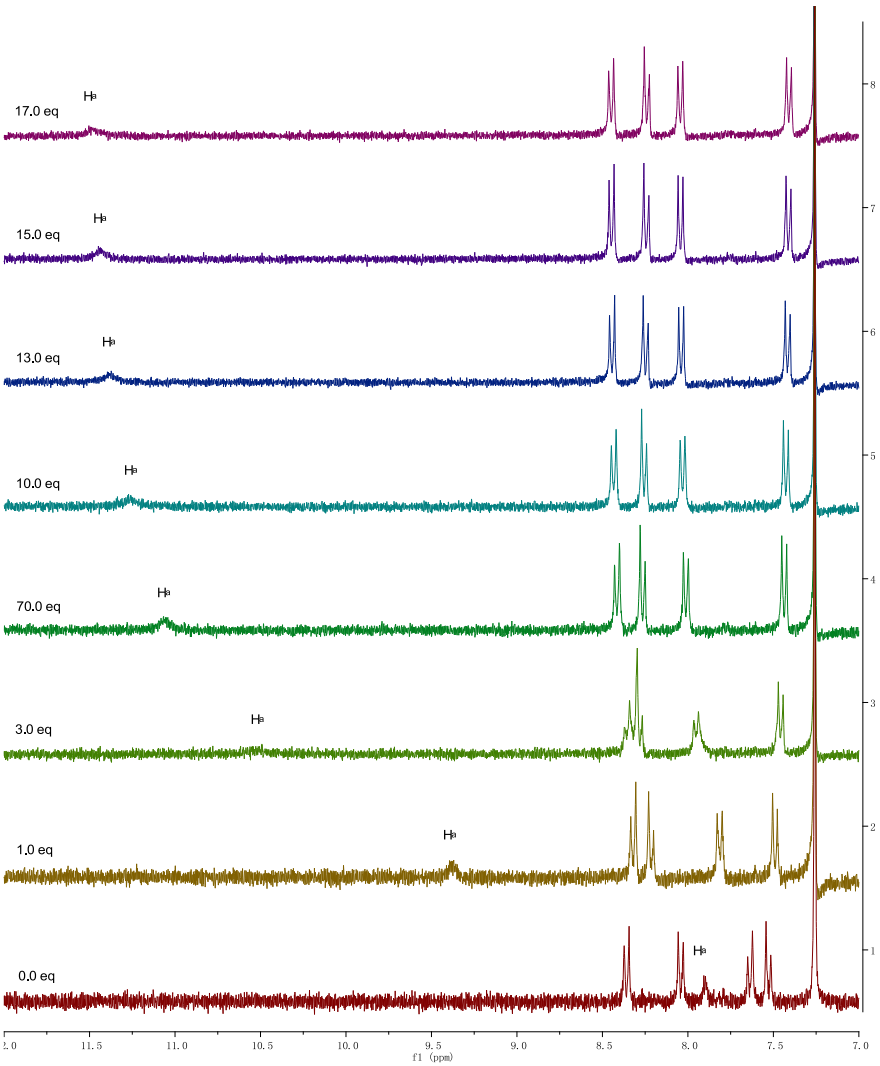

Figure S53. The ^{1}H NMR spectral changes of **4a** upon addition of OAc^{-} in $CDCl_3$ at 298 K.

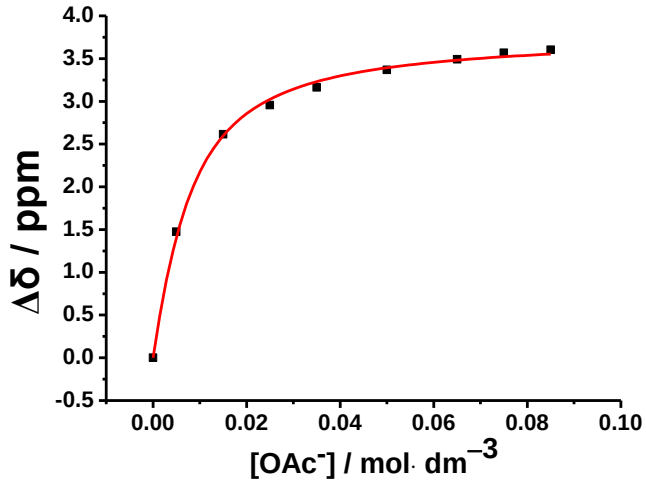

Figure S54. A plot of the chemical shift change of amide proton H_a as a function of [AcO^{-}] and its theoretical fit for the 1:1 binding of **4a** with AcO^{-}.

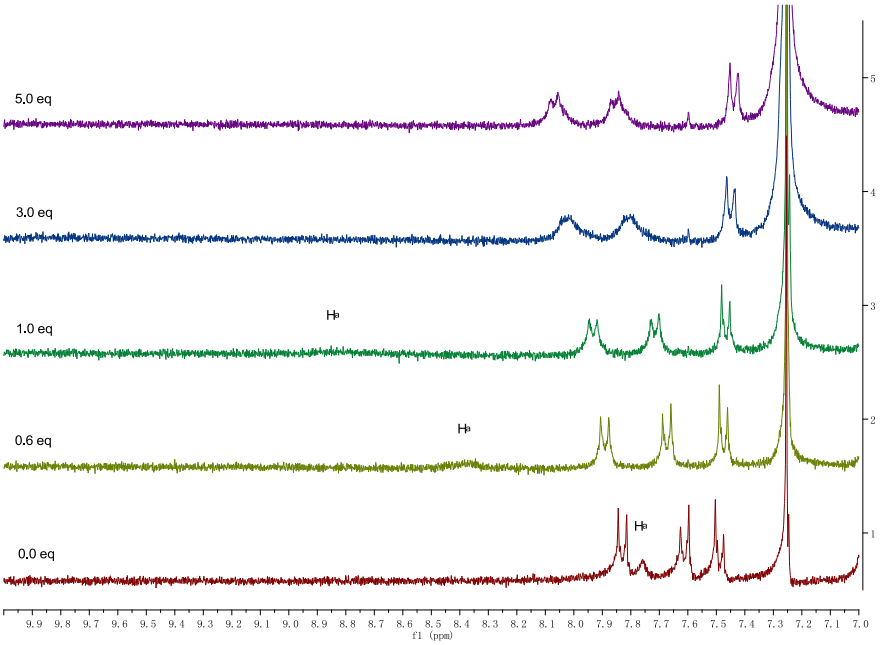

Figure S55. The ^{1}H NMR spectral changes of **4d** upon addition of F^{-} in $CDCl_3$ at 298 K.

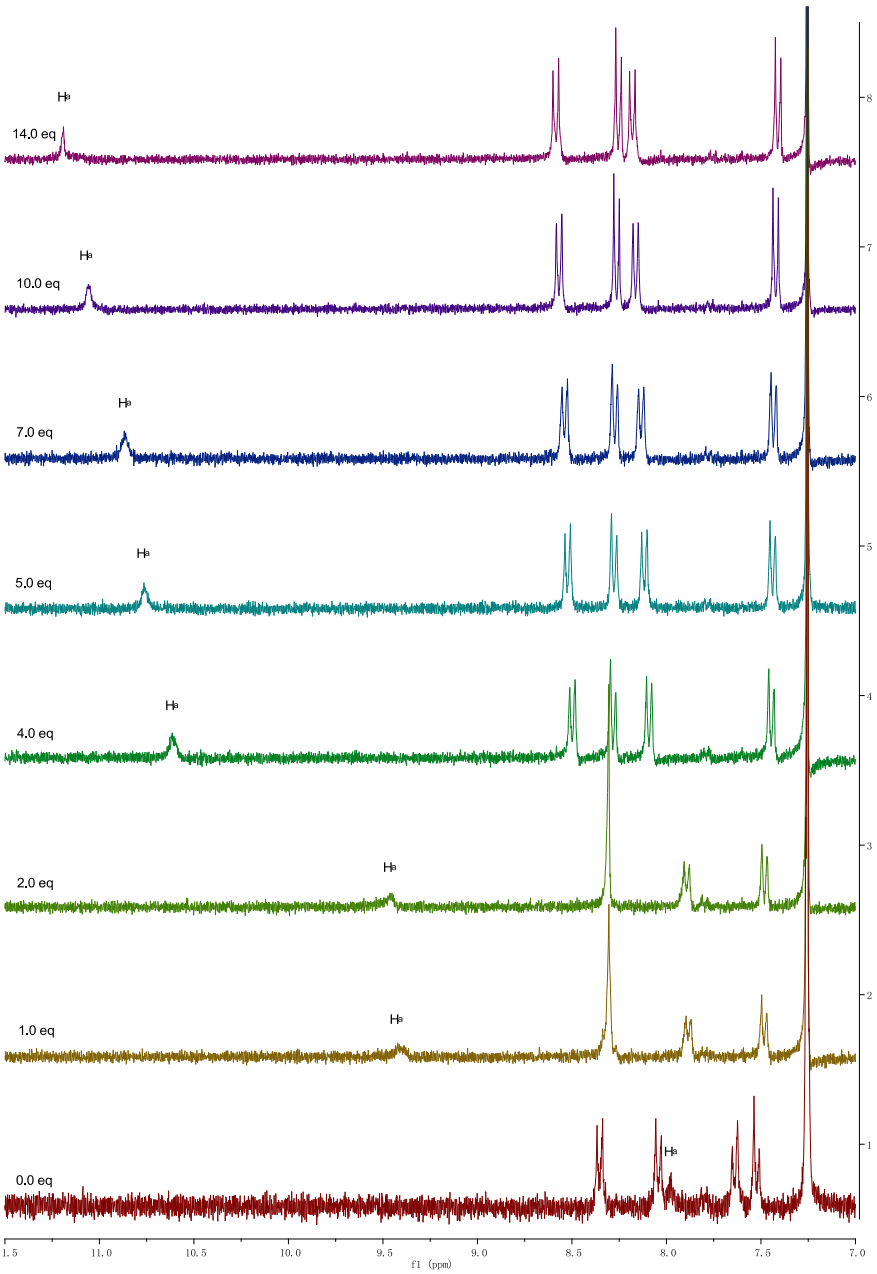

Figure S56. The ^{1}H NMR spectral changes of **4d** upon addition of Cl^{-} in $CDCl_3$ at 298 K.

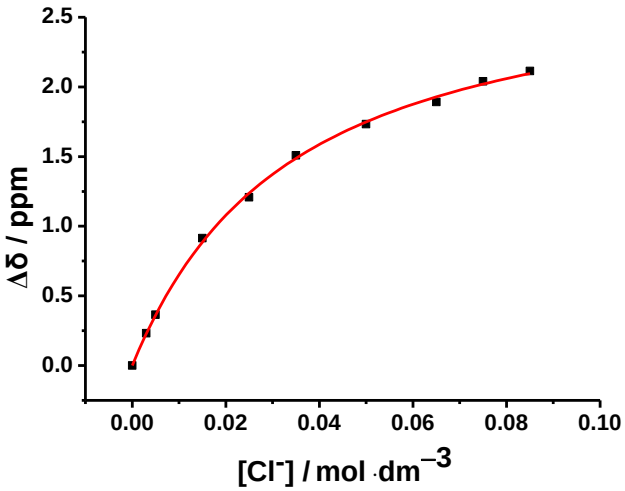

Figure S57. A plot of the chemical shift change of amide proton H_a as a function of [Cl^-] and its theoretical fit for the 1:1 binding of **4d** with Cl^-.

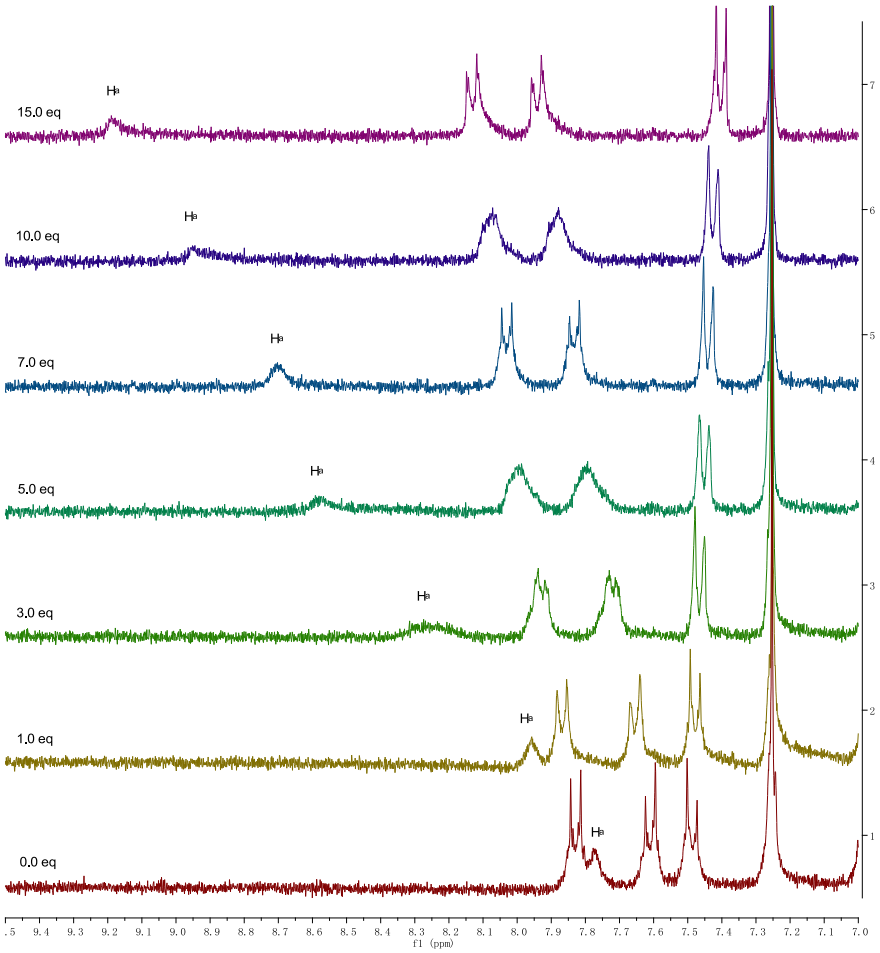

Figure S58. The ^{1}H NMR spectral changes of **4d** upon addition of Br^{-} in $CDCl_3$ at 298 K.

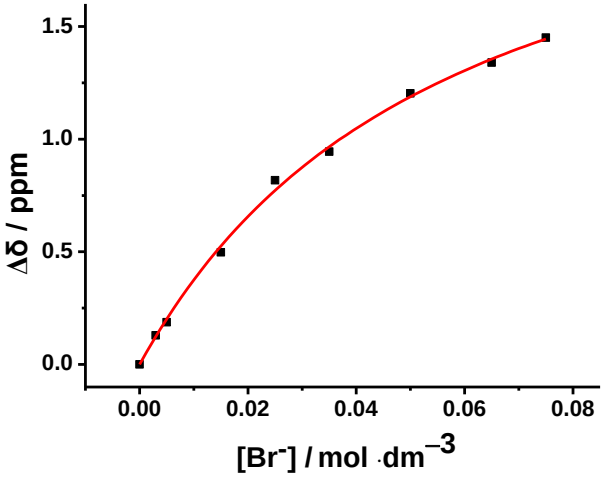

Figure S59. A plot of the chemical shift change of amide proton H_a as a function of [Br^{-}] and its theoretical fit for the 1:1 binding of **4d** with Br^{-}.

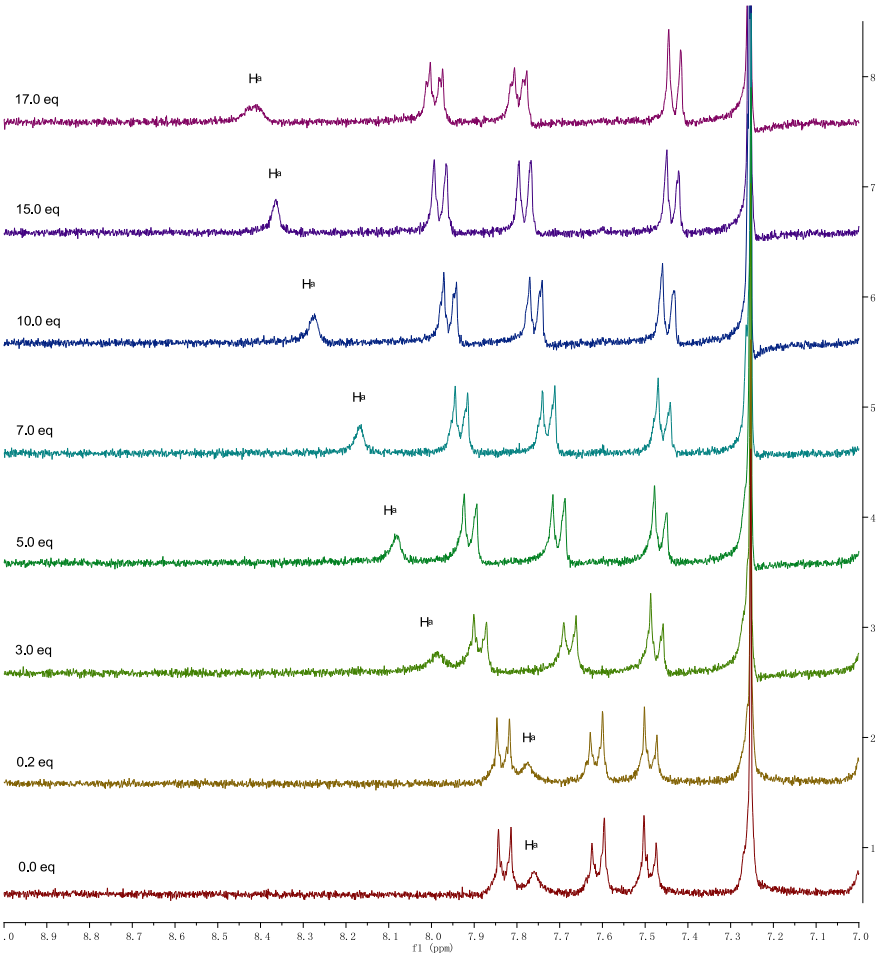

Figure S60. The ^{1}H NMR spectral changes of **4d** upon addition of I^- in $CDCl_3$ at 298K.

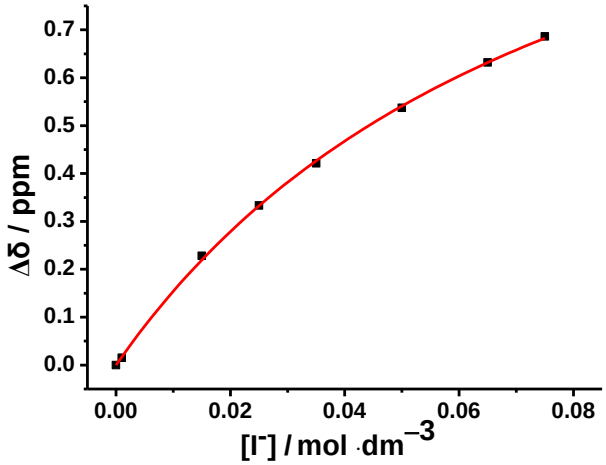

Figure S61. A plot of the chemical shift change of amide proton H_a as a function of [I^-] and its theoretical fit for the 1:1 binding of **4d** with I^-.

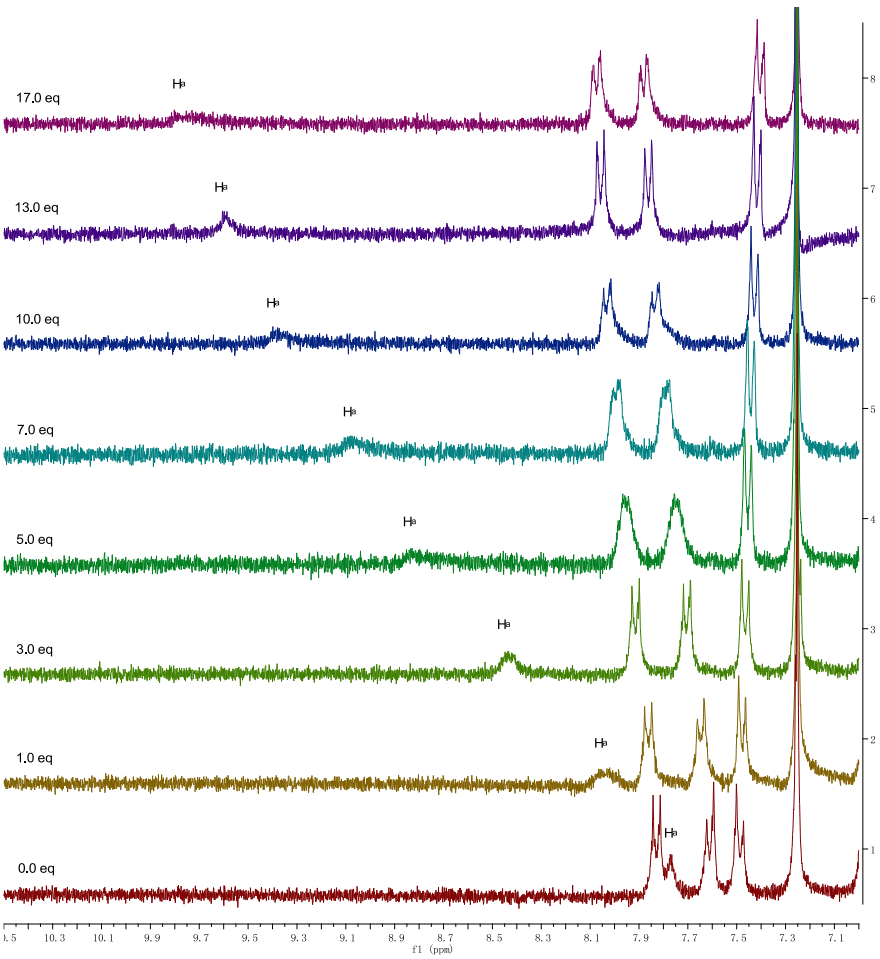

Figure S62. The ^{1}H NMR spectral changes of **4d** upon addition of OAc^{-} in $CDCl_3$ at 298 K.

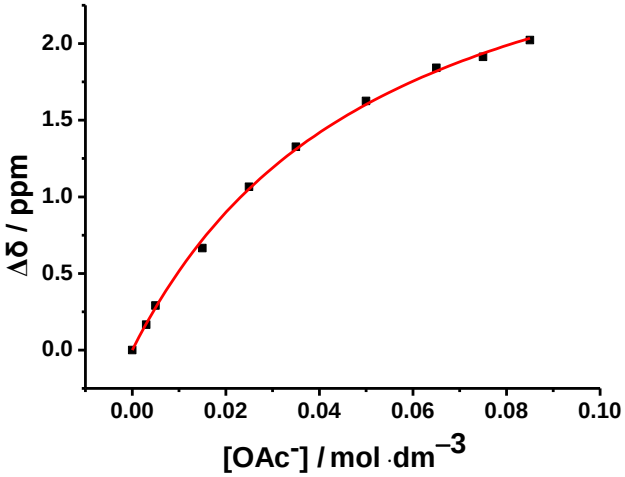

Figure S63. A plot of the chemical shift change of amide proton H_a as a function of [AcO^{-}] and its theoretical fit for the 1:1 binding of **4d** with AcO^{-}.

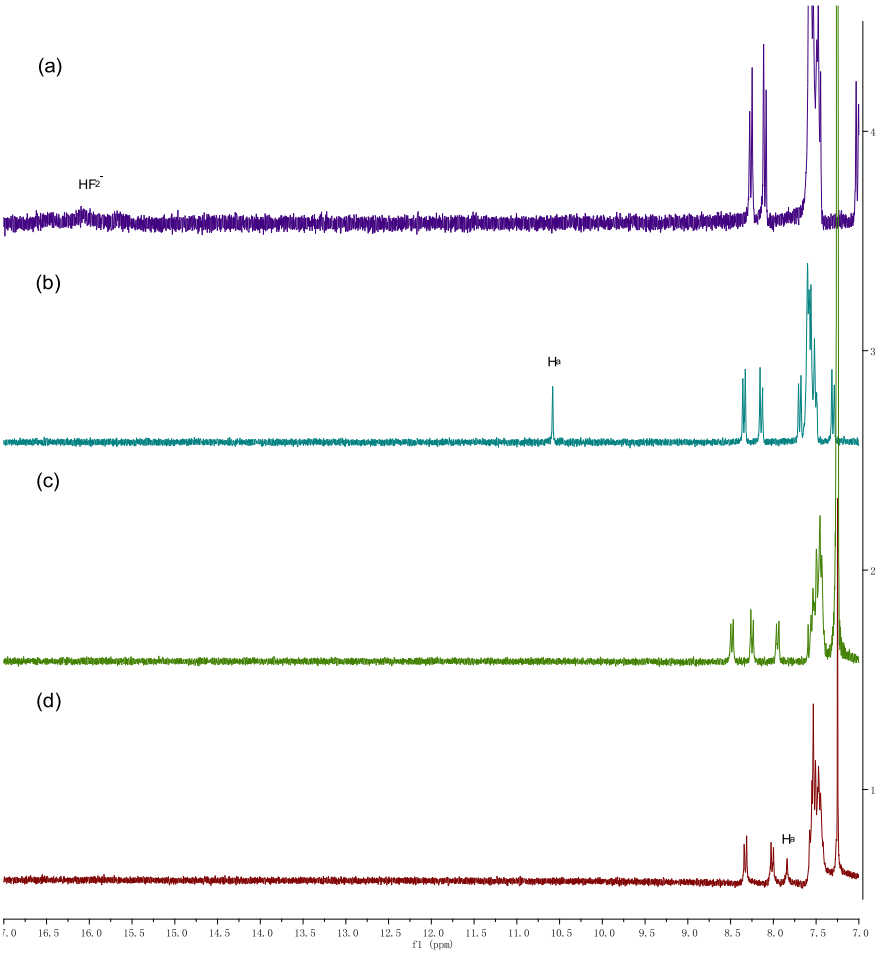

Figure S64. The ^{1}H NMR spectrum of (a) **3a** + 10 eq of F^- (DMSO-d_6, 298 K), (b) **3a** (DMSO-d_6, 298 K),(c) **3a** + 10 eq of F^- ($CDCl_3$, 298 K), and (d) **3a** ($CDCl_3$, 298 K), ([**3a**] = 5.0×10^{-3}mol dm^{-3}).

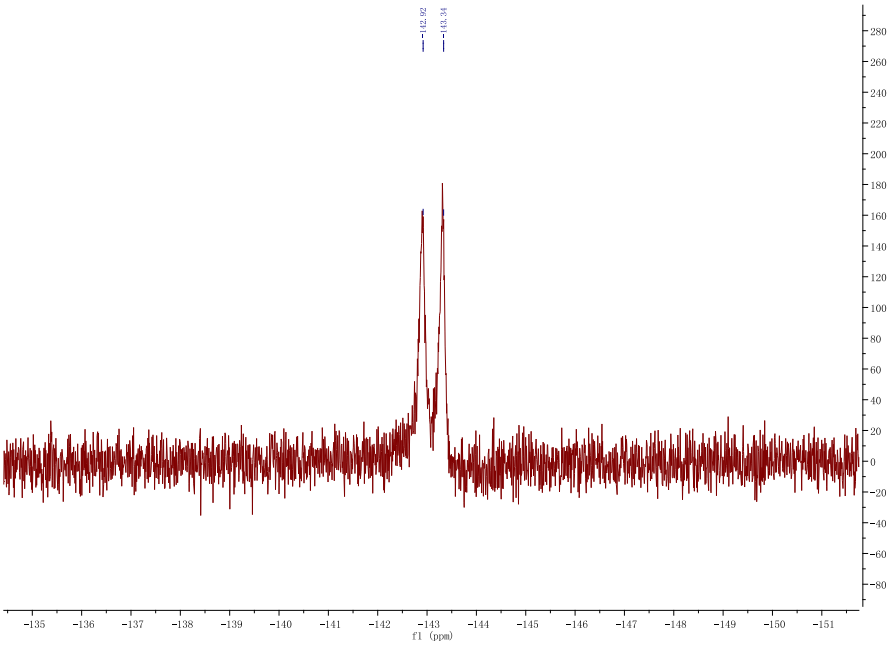

Figure S65. The ^{19}F NMR spectrum of **3a** (5.0×10^{-3}mol dm^{-3}) + 10 eq of F^- in DMSO-d_6 at 298 K.

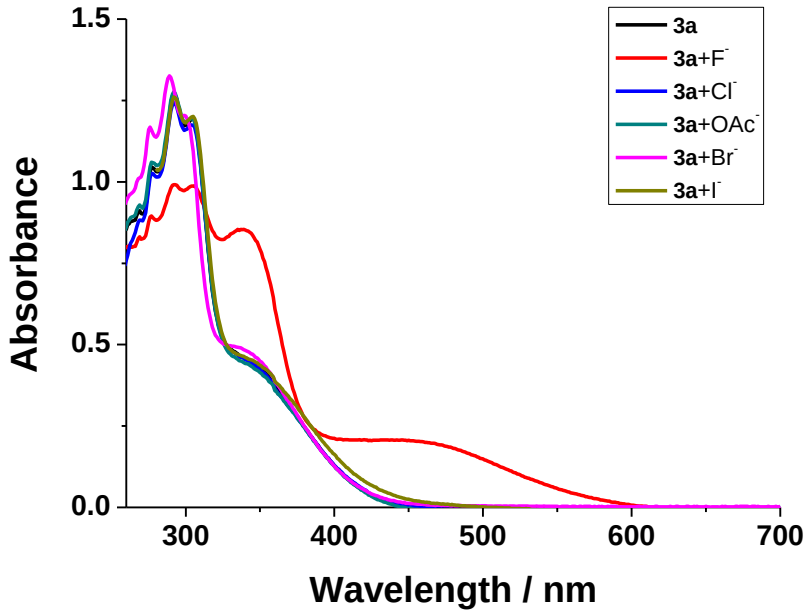

Figure S66. The UV−vis spectra of **3a** (3.96×10^{-5} mol dm^{-3}) in DMSO in the presence of 50 eq of F^-, Cl^-, Br^-, I^-, or OAc^-.

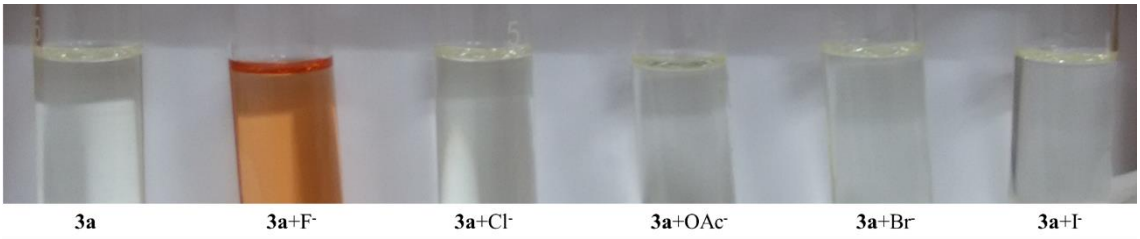

Figure S67. Colors of **3a** (3.96×10^{-5} mol dm^{-3}) in DMSO in the presence of 50 eq of F^-, Cl^-, Br^-, I^-, or OAc^-.